Linking Multiple Bonds between Metal Atoms: Clusters, Dimers of "Dimers", and Higher Ordered Assemblies

Malcolm H. Chisholm*

Department of Chemistry, The Ohio State University, 100 West 18th Avenue, Columbus, Ohio 43210-1185

Ann M. Macintosh*

Department of Physical Sciences, Morehead State University, 123 Lappin Hall, Morehead, Kentucky 40351-1689

Received October 4, 2004

Contents

* Corresponding author information: M.H.C. telephone, 614-292-7216; fax, 614-292-0368; e-mail, chisholm@chemistry.ohio-state.edu. A.M.M. telephone, 606-783-2926; fax, 606-783-5002; e-mail, a.macintosh@morehead-st.edu.

1. Introduction

The concept of multiple bonds is one that owes its origin to Lewis structures and is most applicable to diatomic molecules. It is a bonding model that most chemists cling to dearly, for it has at its root the very concept of an electron pair bond. In molecular orbital theory, the picture becomes much more complicated and even in diatomic molecules such as N_2, which every chemist would agree has a formal triple bond, the detailed nature of the σ molecular orbitals blurs the simplistic but ever so appealing description N≡N.[1] In polyatomic molecules, the concept of localized multiple bonds is still embraced by organic and inorganic chemists. Ketones have C−O double bonds, nitriles have C−N triple bonds, and alkenes and alkynes have C−C double and triple bonds, respectively. Cotton's discovery of the Re−Re quadruple bond in the $Re_2Cl_8^{2-}$ anion marked the recognition of a δ bond[2] and caused the world to recognize a bond of order four, one of higher order than had been seen before. Following this discovery in 1964, the field of multiple bonds between metal atoms has rapidly developed, largely from the work of Cotton and coworkers.[3] Mo_2 was subsequently prepared by matrix isolation, and on the basis of experimental and computational chemistry, it was shown to have a sextuple bond.[4] This remains and will likely remain the record in terms of maximum bond order. However, Mo_2 is not a kinetically stable molecule; it oligomerizes to form Mo(metal). Indeed, with the relatively few exceptions of N_2, CO, and O_2, multiple bonds between elements are thermodynamically unstable with respect to polymerization (or at least oligomerization, as is the case for, say, S_2 to give S_8, P_2 to give P_4, and acetylene to give benzene). The unique stability of multiple bonds between the first row elements (C, N, and O) is a result of their He $1s^2$ core, which favors p−p π-bonding. Thus, it seems that multiple bonds between metal atoms are favored by kinetic factors. They occur in molecules or ions that have sterically encumbered metal centers or are

10.1021/cr980024c CCC: $53.50
Published on Web 07/23/2005

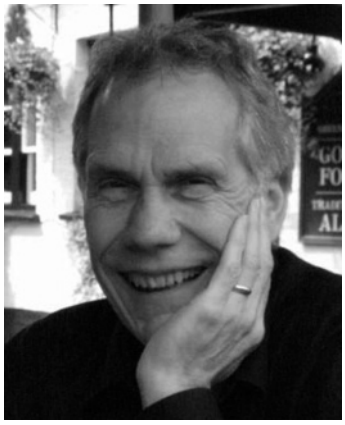

Malcolm H. Chisholm was born in Bombay, India (1945), to Scottish parents and was educated in England, at Canford School and Queen Mary College, London. He received his Ph.D. in 1969 under the direction of Professor D. C. Bradley and did postdoctoral studies at the University of Western Ontario with Professor H. C. Clark. After academic appointments at Princeton University and Indiana University, he assumed his current position at The Ohio State University in 2000, where he is Distinguished Professor of Mathematical and Physical Sciences. His research interests include the chemistry of complexes with metal–metal multiple bonds, the use of alkoxide and related π-donor ligands in organometallic chemistry, molecular routes to materials, and the development of catalysts for the preparation of biodegradable and biocompatible polymers from readily renewable resources. He is author or coauthor of over 500 publications and has received several awards for his research, including the Awards for Inorganic Chemistry and Distinguished Service to Inorganic Chemistry of the American Chemical Society and the Centenary and Ludwig Mond Lectureships of the Royal Society of Chemistry. He is a Fellow of the Royal Society, London, the American Academy of Arts & Sciences, and the German Academy of Natural Sciences—Leopoldina, and he is the recipient of the Davy Medal of the Royal Society. He has served as Associate Editor for the Americas for *Chemical Communications, Dalton Transactions* and as Associate Editor for the inorganic journal *Polyhedron*, and he has held several positions of office within the American Chemical Society, including Chair of the Division of Inorganic Chemistry.

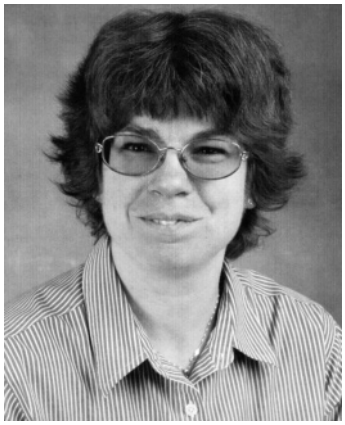

Ann M. Macintosh was born in Barre, MA, in 1968. She received her B.S. degree from Ithaca College in 1990 and her Ph.D. degree with Professor Daniel Nocera from Michigan State University in 1997. From 1997 to 1999, she carried out postdoctoral work with Professor Malcolm Chisholm at Indiana University. She is currently Associate Professor of Chemistry at Morehead State University in Morehead, KY. Her area of research is the photoinduced transformations of inorganic compounds used as artists' pigments.

otherwise prevented from association by charge or ligand constraints. It occurred to one of us several years ago that association of M−M multiply bonded complexes should be possible under certain conditions and that in some instances this might be reversible.[5] Since that time, there have been numerous examples of the dimerization of M−M multiply bonded complexes to give either M_4 clusters or linked dimers of "dimers." In this article, we describe what is known about these systems in terms of their synthesis, structures, and properties.

In terms of organization, we have sorted the complexes into so-called clusters and linked dimers of "dimers", cyclotrimers (triangles), cyclotetramers (squares), higher ordered assemblies, and one-dimensional chains. The other point of organization worthy of comment is that we have elected to employ the parentage of the M_2 starting complexes by metal and bond order. In certain instances, subsequent redox reactions may have occurred such that the number of M−M bonding electrons has changed.

2. M_2 Starting Materials with a Bond Order of 4

2.1. M_4 Clusters

Tetrametallacyclodiynes comprise the largest class of clusters prepared from dinuclear complexes with a metal−metal bond order of four. These clusters are formed when pairs of metal−metal quadruply bonded complexes undergo [2 + 2] cycloaddition with loss of the δ components to leave two triply bonded dinuclear units joined by single M−M bonds along the long edges of the rectangle. The formation of the tetrametallacyclodiynes is shown schematically in Figure 1.

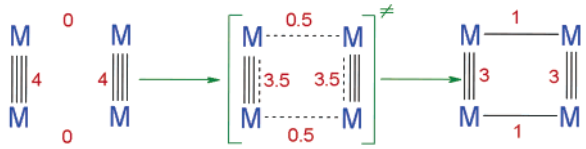

Figure 1. Formation of a tetranuclear cyclodiyne cluster by the [2 + 2] cycloaddition of two M−M quadruply bonded dinuclear units.

2.1.1. Molybdenum and Tungsten

McCarley and co-workers[6] prepared the first cluster of this type, a brown microcyrstalline solid with the empirical formula $[MoCl_2(PPh_3)]_n$, by dissolving $Mo_2Cl_4(PPh_3)_2(CH_3OH)_2$ in benzene at room temperature. A secondary reaction with liberated methanol precluded further characterization of this product. However, subsequent reaction of this species with trialkylphosphines in benzene at 25 °C yielded the crystalline compounds $Mo_4Cl_8(PR_3)_4$, R = C_2H_5 or C_4H_9. Despite the fact that structure determinations on these compounds did not refine especially well, the essential features of the new tetranuclear clusters are clearly defined. Cotton and co-workers[7] later redetermined the structure of $Mo_4Cl_8(PEt_3)_4$, including in the model 8% disorder in which the M_4 rectangle is oriented perpendicular to the main one, and greatly improved the quality of the refinement. The primary part of the structure, shown in Figure 2, is virtually identical to that reported by McCarley et al.; namely, the clusters have a rectangular geometry with effective C_{2h} symmetry. The Mo−Mo bond distances and Mo−Cl−Mo bond angles indicate that the cluster is best described as consisting of Mo−

Mo single bonds along the long edges and Mo−Mo triple bonds along the short edges of the rectangle. Therefore, these new clusters can legitimately be regarded as tetrametal analogues of cyclobutadiyne.

The cycloaddition of $Mo_2Cl_4(PPh_3)_2(MeOH)_2$ can proceed either by the elimination of methanol to produce $Mo_4Cl_8(PPh_3)_4$ or by the loss of triphenylphosphine to yield $Mo_4Cl_8(MeOH)_4$, depending on the reaction conditions,[8] as shown in eqs 1 and 2. The

$$2Mo_2Cl_4(PPh_3)_2(MeOH)_2 \rightarrow Mo_4Cl_8(PPh_3)_4 + 4MeOH \quad (1)$$

$$2Mo_2Cl_4(PPh_3)_2(MeOH)_2 \rightarrow Mo_4Cl_8(MeOH)_4 + 4PPh_3 \quad (2)$$

loss of methanol is favored in benzene solutions while the loss of PPh_3 is promoted in a two-phase methanol/cyclohexane solvent system. The cycloaddition process is facilitated by the unusual lability of the PPh_3 and CH_3OH ligands in this "activated dimer". While the exact mechanism of the cycloaddition reaction is not known, it is thought that the reaction is initiated by dissociation of coordinated ligands from the dinuclear complex. The resulting species of low coordination number are unstable and readily condense to form tetranuclear clusters. The tetranuclear $Mo_4Cl_8(MeOH)_4$ species can easily be converted back to quadruply bonded "dimers" upon addition of an excess of a donor ligand.[8] Because of secondary reactions involving liberated methanol, vide supra, $Mo_4Cl_8(PPh_3)_4$ must be synthesized by an indirect route.[8] The $Mo_4Cl_8(PPh_3)_4$ cluster is best prepared from the reaction between $Mo_4Cl_8(EtCN)_4$ and PPh_3. The $Mo_4Cl_8(EtCN)_4$ cluster is, in turn, prepared by stirring $Mo_4Cl_8(MeOH)_4$ in propionitrile for 24 h.

Several additional synthetic routes to $Mo_4Cl_8(PR_3)_4$ clusters, shown in eqs 3−6, have been developed,[8]

$$2K_4Mo_2Cl_8 + 4PR_3 \xrightarrow[MeOH]{\Delta} Mo_4Cl_8(PR_3)_4 + 8KCl \quad (3)$$

$$2Mo_2(O_2CCH_3)_4 + 8Me_3SiCl + 4PR_3 \xrightarrow[THF]{\Delta} Mo_4Cl_8(PR_3)_4 + 8Me_3Si(O_2CCH_3) \quad (4)$$

$$2Mo_2(O_2CCH_3)_4 + 4AlCl_3 + 4PR_3 \xrightarrow[THF]{\Delta} Mo_4Cl_8(PR_3)_4 + 4AlCl(O_2CCH_3)_2 \quad (5)$$

$$2Mo_2Cl_4(PR_3)_4 + 2Mo(CO)_6 \xrightarrow[THF]{\Delta} Mo_4Cl_8(PR_3)_4 + 2Mo(CO)_4(PR_3)_2 + 4CO \quad (6)$$

which has led to a greater variety of clusters and, in some cases, improved yields. Clusters with $R_3 = Me_3$, $^nPr_3$, and Me_2Ph, in addition to $R_3 = Et_3$, $^nBu_3$, and Ph_3 previously reported, were prepared using these new synthetic methods. The $Mo_4Cl_8(PR_3)_4$ (R = alkyl) clusters are soluble in common organic solvents and are only slightly air-sensitive. The bromo and iodo analogues of these clusters were also prepared[8] by reacting $Mo_2(O_2CCH_3)_4$ with the appropriate trimethylsilyl halide in the presence of a trialkylphosphine (eq 7). A comparison of the X-ray powder

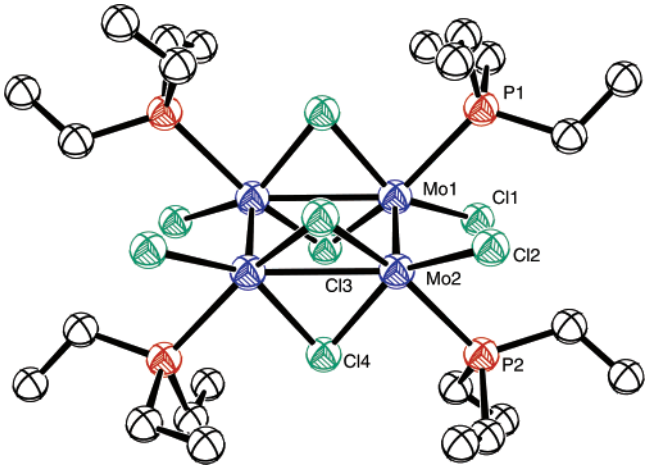

Figure 2. Molecular structure of $Mo_4Cl_8(PEt_3)_4$. Hydrogen atoms are omitted for clarity. Only one set of symmetry-equivalent atoms is labeled.

$$2Mo_2(O_2CCH_3)_4 + 8Me_3SiX + 4PR_3 \xrightarrow[THF]{\Delta} Mo_4X_8(PR_3)_4 + 8Me_3Si(O_2CCH_3) \quad (7)$$

patterns and electronic spectra of the Br and Cl analogues of $Mo_4X_8(PBu_3)_4$ strongly indicates that the two clusters have very similar structures. In contrast, the electronic spectrum of $Mo_4I_8(PBu_3)_4$ suggests that the complex does not have the same electronic structure as that of the chloro and bromo analogues, vide infra.

A tetramolybdenumcyclodiyne cluster with trimethyl phosphite instead of a phosphine can also be prepared[9] either by reacting $K_4Mo_2Cl_8$ with $P(OMe)_3$ or by refluxing $Mo_2Cl_4(P(OMe)_3)_4$ in methanol. The structure of $Mo_4Cl_8(P(OMe)_3)_4$ is quite similar to those reported previously for $Mo_4Cl_8(PR_3)_4$ where R = alkyl. The bond distances and bond angles in $Mo_4Cl_8(P(OMe)_3)_4$ compare favorably with those reported for $Mo_4Cl_8(PEt_3)_4$.

Tetramolybdenumcyclodiynes containing bidentate phosphine ligands can be synthesized[10] using a procedure slightly modified from the one used for the preparation of $Mo_4Cl_8(PR_3)_4$ complexes with monodentate phosphines. Specifically, when $K_4Mo_2Cl_8$ was refluxed in methanol for 24−36 h, followed by the addition of 1 equiv of dppm (bis(diphenylphosphino)-methane), $Mo_4Cl_6(OMe)_2(dppm)_2$ was formed. This reaction is thought to proceed according to eq 8.

$$2K_4Mo_2Cl_8 + 6MeOH \xrightarrow[24-36\ H]{\Delta} Mo_4Cl_4(\mu\text{-}Cl)_2(\mu\text{-}OMe)_2(MeOH)_4 + 8KCl + 2HCl$$
$$\downarrow 2\ dppm$$
$$Mo_4Cl_4(\mu\text{-}Cl)_2(\mu\text{-}OMe)_2(\mu\text{-}dppm)_2 + 4MeOH \quad (8)$$

The four Mo atoms in this cluster define a rectangle; each long Mo−Mo bond is bridged by one methoxy group and one Cl atom, while each short Mo−Mo bond is bridged by one dppm ligand. The Mo−Mo distances and Mo−Cl−Mo and Mo−O−Mo bond angles are consistent with the existence of Mo−Mo single bonds along the long edges and Mo−Mo

triple bonds on the short edges of the rectangle. However, when dmpm (bis(dimethylphosphino)-methane) is substituted for dppm, the same synthetic procedure yields $Mo_4Cl_7(\mu_4\text{-}O)(OMe)_3(dmpm)_2$ rather than the expected product.[10] The $Mo_4Cl_7(\mu_4\text{-}O)(OMe)_3(dmpm)_2$ cluster features a Mo_4 rectangle capped by an μ_4-O atom. The two Mo−Mo triple bonds are each bridged by one dmpm ligand and one methoxy group. One of the Mo−Mo single bonds is bridged by one Cl atom and one methoxy group while the other is bridged by two Cl atoms.

The W_4 and Mo_2W_2 congeners of the tetrametallacyclodiynes have also been synthesized.[11,12] The $W_4Cl_8(PBu_3)_4$ cluster was prepared by using the synthetic methodology developed by Schrock and coworkers;[13] the procedure is summarized in eqs 9−11.

$$2WCl_4 + 2Na(Hg) \xrightarrow{THF} W_2Cl_6(THF)_4 + 2NaCl \quad (9)$$

$$W_2Cl_6(THF)_4 + 2P^nBu_3 \xrightarrow{THF} W_2Cl_6(THF)_2(P^nBu_3)_2 + 2THF \quad (10)$$

$$W_2Cl_6(THF)_2(P^nBu_3)_2 + 2Na(Hg) \xrightarrow{THF} W_4Cl_8(P^nBu_3)_4 + 2NaCl \quad (11)$$

The W_4 cluster[11] has D_2 symmetry, which differs from that of $Mo_4Cl_8(PEt_3)_4$. However, the essential features of the bonding are quite similar in the two cases. The W_4 cluster is closer in shape to square than its Mo_4 congener; the long bonds of the rectangle are shorter, and the short bonds are longer. The Mo_2W_2 analogues[12] were synthesized by reacting $MoW(O_2C^tBu)_4$ with $AlCl_3$ in the presence of PR_3; R = CH_3 or ^{n}Bu. The metal−metal bonding within the Mo_2W_2 clusters more closely resembles that of $W_4Cl_8(PBu_3)_4$ than that of $Mo_4Cl_8(PBu_3)_4$. The ^{31}P NMR spectrum of $Mo_2W_2Cl_8(PBu_3)_4$ reveals the presence of two isomers, head-to-head and head-to tail, in a 1.5 to 1 ratio.

The $Mo_4Cl_8(PR_3)_4$ clusters can undergo coupling reactions[14] to build up even larger clusters. The reaction of tetramolybdenumcyclodiynes with $Mo(CO)_6$ in refluxing chlorobenzene results in the abstraction of phosphine and the formation of condensation products of composition $[Mo_4Cl_8(PR_3)_2]_x$. The condensation product, $[Mo_4Cl_8(PEt_3)_2]_x$, reacts with excess PEt_3 in hot chlorobenzene to yield $Mo_2Cl_4(PEt_3)_4$. Alternatively, if up to 2 equiv of PEt_3 is added dropwise to a refluxing suspension of $[Mo_4Cl_8(PEt_3)_2]_x$, the predominant product is $Mo_4Cl_8(PEt_3)_4$. The reactivity of $[Mo_4Cl_8(PEt_3)_2]_x$ suggests that the rectangular cluster units are essentially preserved in the condensation products, coupled together solely through Mo−Cl−Mo bridges. On the basis of the fact that the condensation products are microcrystalline and exhibit significant solubility in noncoordinating solvents, it was proposed that these compounds are best described as dimers of tetramers rather than polymers. However, a reactive form of β-$MoCl_2$, prepared from the reaction between $Mo_2(O_2CMe)_4$ and $AlCl_3$, has been described as a polymer of M_4 units bridged by Cl ligands.[15]

2.1.2. Rhenium

Initial attempts to expand the chemistry of the tetrametallacyclodiynes to include Re_4 rings bridged by Cl atoms were unsuccessful. Cotton and coworkers subsequently prepared $(Bu_4N)_2Re_4Cl_8(\mu\text{-}Cl)(\mu\text{-}O)_2(\mu\text{-}OMe)$[16] by refluxing $(^nBu_4N)_2Re_2Cl_8$ in a mixture of MeOH and H_2O. The four Re atoms of the cluster define a rectangle; one of the long Re−Re bonds is bridged by one oxo and one methoxy group, while the other is bridged by one oxo group and one Cl atom; and each Re atom is coordinated by two terminal Cl ligands. The Re−Re bond distances and Re−O−Re and Re−Cl−Re bond angles are all consistent with the presence of two Re−Re single bonds and two Re−Re triple bonds.

The closely related complex $(^nBu_4N)_2Re_4Cl_8(\mu\text{-}O)_2(\mu\text{-}OMe)_2$ was obtained unexpectedly from the reaction of $(^nBu_4N)_2Re_2Cl_8$ and (+)-BINAP in refluxing methanol.[16] The structure of $(^nBu_4N)_2Re_4Cl_8(\mu\text{-}O)_2(\mu\text{-}OMe)_2$ is very similar to that of $(Bu_4N)_2Re_4Cl_8(\mu\text{-}Cl)(\mu\text{-}O)_2(\mu\text{-}OMe)$ with the exception of the fact that the μ-Cl atom has been replaced by a bridging methoxy group. The third member of this series, $(^nBu_4N)_2[Re_4Cl_8(\mu\text{-}Cl)_2(\mu\text{-}O)_2\cdot THF]$, was prepared by refluxing

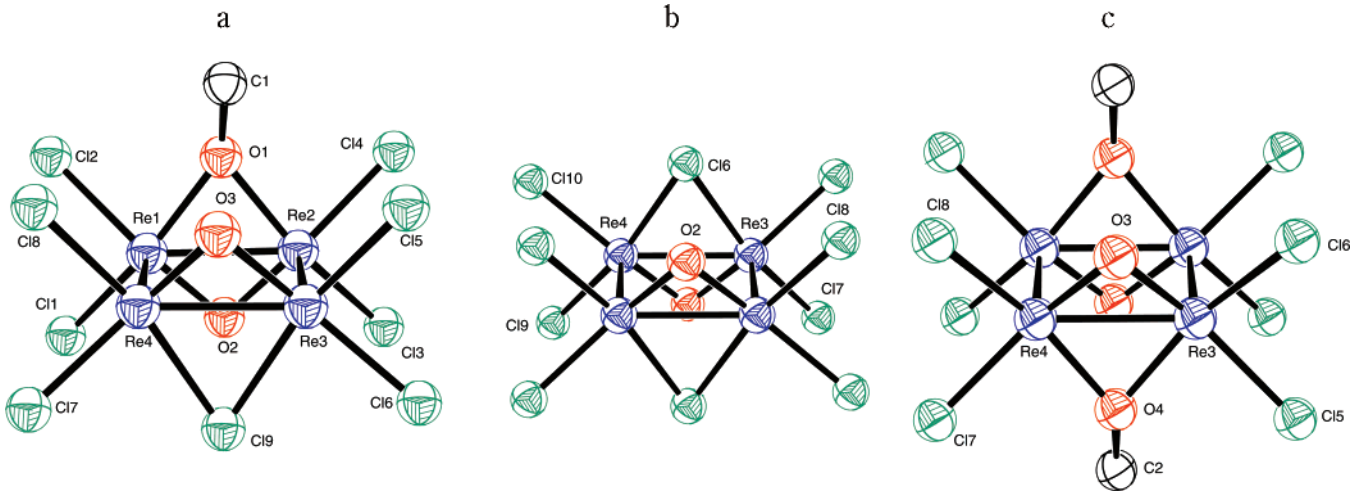

Figure 3. Re_4-containing fragments of (a) $[Bu_4N]_2[Re_4Cl_8(\mu_2\text{-}Cl)(\mu_2\text{-}O)_2(\mu_2\text{-}OMe)]$, (b) $[Bu_4N]_2[Re_4Cl_8(\mu_2\text{-}Cl)_2(\mu_2\text{-}O)_2]\cdot THF$, and (c) $[Bu_4N]_2[Re_4Cl_8(\mu_2\text{-}O)_2(\mu_2\text{-}OMe)_2]$. The THF molecule is omitted from part b, and methyl hydrogen atoms are omitted for clarity in parts b and c. Only one set of symmetry equivalent atoms is labeled for each anion.

$(^nBu_4N)_2Re_2Cl_8$ in wet trifluoroacetic acid.[17] The complex is isostructural with the other two complexes in the series; the two μ-Cl atoms are located trans to each other. The structures of the three clusters are shown for comparison in Figure 3.

Walton and co-workers[18] prepared the first example of a neutral, symmetrical, tetrarheniumcyclodiyne cluster containing phosphine ligands, $Re_4(\mu\text{-}O)_4Cl_4[P(C_6H_4OMe\text{-}p)_3]_4$, by reacting $Re_2(O_2CCH_3)_2Cl_4(H_2O)_2$ with $P(C_6H_4OMe\text{-}p)_3$ in methanol. Under the same reaction conditions, $Re_2(O_2CCH_3)_2Cl_4(H_2O)_2$ reacts with other PAr_3 molecules (Ar = Ph, C_6H_4Me-*p*, C_6H_4Me-*m*, or C_6H_4Cl-*p*) to yield quadruply bonded dirhenium(IV,II) dinuclear complexes of the type $Re_2(OMe)_2Cl_4(PAr_3)_2$.[18] The diamagnetic $Re_4(\mu\text{-}O)_4Cl_4[P(C_6H_4OMe\text{-}p)_3]_4$ complex was characterized by X-ray crystallography and shown to contain a rectangular cluster of metal atoms with two Re−Re single bonds. Formally, this cluster arises from the [2 + 2] cycloaddition of two Re−Re quadruply bonded dinuclear units. Two other $Re_4(\mu\text{-}O)_4Cl_4(PR_3)_4$ complexes were prepared by using other synthetic methods. The tetranuclear $Re_4(\mu\text{-}O)_4Cl_4(PPh_3)_4$ was prepared by refluxing $Re_2(O_2CCH_3)Cl_4(PPh_3)_2$ and $LiOH\cdot 2H_2O$ in methanol. Additionally, $Re_4(\mu\text{-}O)_4Cl_4(PMe_2Ph)_4$ was prepared by reacting PMe_2Ph with $Re_4(\mu\text{-}O)_4Cl_4[P(C_6H_4OMe\text{-}p)_3]_4$ in dichloromethane.[19] The formation of this Re_4 cluster is analogous to that of the Mo_4 clusters prepared by McCarley et al.[6−10]

2.2. Dimers of "Dimers"

2.2.1. Halide-Bridged Complexes of Molybdenum

In addition to the tetrametallacyclodiynes, there are also several examples of clusters in which two quadruply bonded dinuclear complexes are joined together in the shape of a rectangle by means of four bridging halide ligands, with full retention of the two quadruple bonds and no additional M−M bond formation. The crystal structure of $Mo_4I_8(PBu_3)_4$,[20] shown in Figure 4, was solved by Cotton and coworkers and found to differ significantly from those of its Cl and Br analogues, as was predicted on the basis of its electronic spectrum, vide supra. The $Mo_4I_8(PBu_3)_4$ cluster is unique among the $Mo_4X_8(PR_3)_4$ clusters in that it retains the two quadruple bonds as opposed to forming a tetrametallacyclobutadiyne. The iodo analogue is best described as two

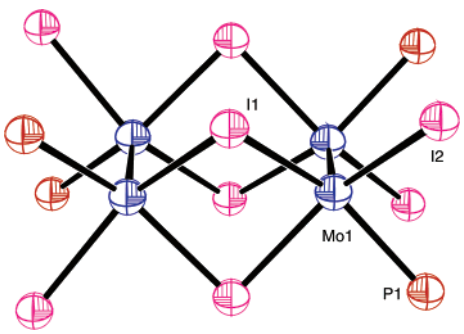

Figure 4. Molecular structure of $Mo_4I_8(P^nBu_3)_4$. The unique part of the molecule is labeled; all other atoms are generated by 222 site symmetry.[20] The phosphine *n*-butyl groups have been omitted for clarity.

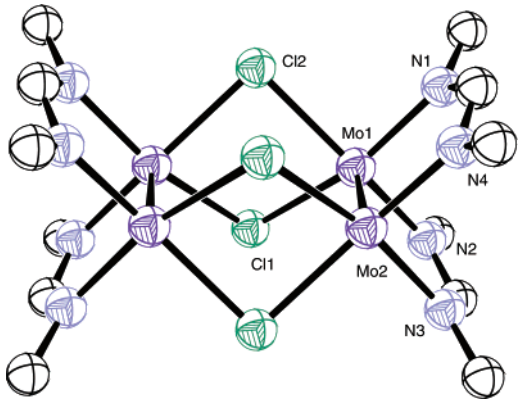

Figure 5. Molecular structure of $[Mo_2(DAniF)_2]_2(\mu\text{-}Cl)_4$. Hydrogen atoms and DAniF anisole groups are omitted for clarity.

independent quadruply bonded dinuclear units linked by four iodo bridges. The larger iodine atoms prevent closer approach of the dinuclear units and, therefore, the formation of the tetrametallacyclodiyne.

A series of clusters that consists of $Mo_2(DArF)_2$ subunits (DArF = ArNC(H)NAr; Ar = *p*-anisyl, *p*-tolyl, and *p*-fluorophenyl) linked by halide bridges has been synthesized and shown to have structures qualitatively similar to that of $Mo_4I_8(PBu_3)_4$ but with bridging formamidinate ligands in place of the terminal halide and phosphine ligands. The $Mo_4Cl_4(DArF)_4$ clusters are prepared by reducing $Mo_2(DArF)_3Cl_2$ with KC_8 in the presence of $ClSiMe_3$.[20] The $Mo_4Cl_4(DArF)_4$ (DArF = ArNC(H)NAr; Ar = *p*-anisyl, *p*-tolyl, and *p*-fluorophenyl) and $Mo_4I_4(DArF)_4$ (Ar = *p*-anisyl) have been structurally characterized. The structure of $Mo_4(DAniF)_4Cl_4$ is shown in Figure 5. The structures of the four complexes are all similar. The four Mo atoms define a rectangle. The short Mo−Mo bond distances are within the established range for Mo−Mo quadruple bonds, while the long Mo···Mo distances are well outside the bonding range. The Mo−Cl−Mo bond angles are ~90°, in marked contrast to those of the tetrametallacyclodiynes, which range from 72 to 74°.[20]

Cotton has shown that this chloride-bridged complex can be oxidized to give a delocalized radical cation where the two dinuclear Mo_2 units have a formal bond order of 3.75 and a M−M distance of 2.1453(3) Å, compared with the case of the neutral compound, with M−M = 2.1191(4) Å and a bond order of 4.[21] The delocalization of the unpaired electron was also evident by EPR spectroscopy.

The reactions between $Mo_2(DArF)_4$ and Me_3SiX (2 equiv) in CH_2Cl_2 at room temperature provide effective routes to $[Mo_2(DArF)_2]_2(\mu\text{-}X)_4$ compounds where X = Br and I.[20] The structure of the iodo complex was determined and revealed the presence of two localized MM quadruple bonds of distance 2.1171(1) Å, supported by the four iodo bridges.

2.2.2. Hydroxo-, Oxo-, and Hydrido-Bridged Complexes of Molybdenum

Dimers of "dimers" in which two $Mo_2(form)_3^+$ units are linked by two hydride-, two hydroxo-, or two oxo-bridges are also known. The different products within this group are obtained by varying the condi-

tions for the reduction of the $Mo_2(DArF)_3Cl_2$ (Ar = *p*-tolyl or *p*-anisyl) starting material. The hydride complex $[Mo_2(DArF)_3]_2(\mu\text{-}H)_2$ was obtained by reducing $Mo_2(DArF)_3Cl_2$ with $NaHBEt_3$ in THF.[20,22] The hydride-bridged complexes have been characterized crystallographically. The Mo−Mo distances are consistent with the presence of Mo−Mo quadruple bonds. Mo−H−Mo angles of ~147° and 144° are similar to those observed in other species containing bridged three-center, two-electron (3c−2e) bonds, and all four Mo atoms and both H atoms are essentially coplanar. The electronic spectra of $[Mo_2(DArF)_3]_2(\mu\text{-}H)_2$ each contain three features: (1) a shoulder at 444, 449 nm, (2) a shoulder at 505 nm in both complexes, and (3) a Gaussian band at 728, 729 nm. The shoulder at 444, 449 nm was assigned as the $\delta \rightarrow \delta^*$ on the basis of the fact that it occurs at similar energy to the $\delta \rightarrow \delta^*$ transition in $Mo_2(DArF)_4$ compounds. As a general rule, for compounds containing M−M quadruple bonds, it is assumed that the lowest energy transition is $\delta \rightarrow \delta^*$. However, that assumption is not reasonable in this particular case. The two lower energy bands have been tentatively assigned as $\delta \rightarrow$ nb and $\delta \rightarrow$ ab, where nb and ab are the nonbonding and antibonding orbitals associated with the Mo−H−Mo bridges, respectively.[22]

If potassium amalgam is used as reducing agent instead of $NaHBEt_3$, the hydroxo-bridged species, $[Mo_2(DTolF)_3]_2(\mu\text{-}OH)_2 \cdot n$-hexane is obtained.[20,23] The two $Mo_2(DTolF)_3$ units are related by a crystallographic inversion center and are joined together by two bridging OH groups. The Mo−Mo distance of 2.107 Å is consistent with the presence of a quadruply bonded Mo_2^{4+} unit. Even though the hydrogen atoms of the μ-OH groups were not observed crystallographically, the relatively long Mo−O distances support the formulation of the bridging groups as OH groups rather than O atoms. The electronic spectrum of $[Mo_2(DTolF)_3]_2(\mu\text{-}OH)_2$ is qualitatively similar to that of $[Mo_2(DArF)_3]_2(\mu\text{-}H)_2$. The $\delta \rightarrow \delta^*$ transition appears as a shoulder at 432 nm. In addition, there are two transitions observed at lower energy than the $\delta \rightarrow \delta^*$ transition, which are related to the Mo−(OH)−Mo bridges.[23]

If the reaction conditions used for the preparation of $[Mo_2(DTolF)_3]_2(\mu\text{-}OH)_2$ are modified such that oxygen is allowed into the system, a mixture of $\{[Mo_2(DTolF)_3]_3(MoO_4)_2\}^-$ anion and $[Mo_2(DTolF)_3]_2(\mu\text{-}O)_2$ is obtained.[20] The oxo-bridged dimer of "dimers" can be prepared in nearly quantitative yields by the air oxidation of $[Mo_2(DTolF)_3]_2(\mu\text{-}OH)_2$ solutions.[20] The Mo−O bond distances in $[Mo_2(DTolF)_3]_2(\mu\text{-}O)_2$, 1.925 and 1.912 Å, are ~0.2 Å shorter than those in $[Mo_2(DTolF)_3]_2(\mu\text{-}OH)_2$. The Mo−Mo distance of 2.140 Å is longer than that in $[Mo_2(DTolF)_3]_2(\mu\text{-}OH)_2$ but similar to the Mo−Mo distance in $Mo_2(DArF)_3Cl_2$, 2.15 Å. The increase in the Mo−Mo distance is due to the oxidation of the quadruply bonded Mo_2^{4+} units to Mo_2^{5+} units, which decreases the bond order to 3.5. In contrast to the hydride- and hydroxide-bridged compounds where all four molybdenum atoms and both bridging atoms are essentially coplanar, the Mo−O−O−Mo torsion angle is ~14°.

2.2.3. Dicarboxylate-Linked Complexes of Molybdenum and Tungsten

An extensive series of dicarboxylate-linked M_2 quadruply bonded complexes has now been prepared, largely as a result of the independent work in the Chisholm[24−34] and Cotton groups.[35−40] The former workers employed the use of the carboxylate group exchange reaction[24] shown in eq 12, which has

$$2[M_2(O_2C^tBu)_4] + HO_2C{-}X{-}CO_2H \xrightarrow[25\ ^\circ C,\ 7\ days]{\text{toluene}} [(^tBuCO_2)_3M_2]_2(\mu\text{-}O_2CXCO_2) \quad (12)$$

limitations based on equilibria and the possibility of higher order oligomers being formed by further substitution.[26,41] Nevertheless, an extensive series of complexes has been prepared and characterized in this manner for both M = Mo and W. The resultant dimers of "dimers" formed in eq 12 are isolated on the basis of the differences in their solubility with respect to the starting materials and products of further substitution.

The Cotton procedure[38] is outlined in eq 13 and has the advantage of employing the kinetically persistent formamidinate (form) ligands, typically anisyl−

$$2[Mo_2(form)_3Cl_2] + Q^+[O_2C{-}X{-}CO_2]^{2-} + NaHBEt_3 \xrightarrow[25\ ^\circ C]{CH_3CN/CH_2Cl_2} [(form)_3Mo_2]_2(\mu\text{-}O_2C\text{-}X\text{-}CO_2)$$
$$\text{where } Q^+ = [N^nBu_4]^+, [NEt_4]^+ \text{ or } Na^+ \quad (13)$$

NC(H)N−anisyl, which are not subject to facile intermolecular ligand-scrambling reactions.[41] This reaction is, however, limited to the preparation of compounds of molybdenum. Variations of this reaction pathway have involved the use of $Mo_2(form)_3(CH_3CN)_2^+$ cations.[35−38]

Particular interest in this class of compounds arises from the electronic coupling between the two M_2 centers by a conjugated bridge. Consequently, the

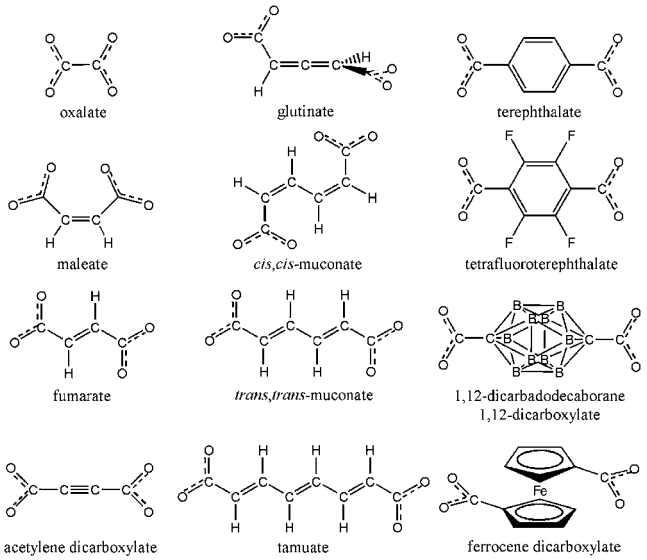

Figure 6. Examples of $O_2C{-}X{-}CO_2$ bridging dicarboxylates.

ligand bridges shown in Figure 6 have been employed. The key orbital interactions involve the M_2 δ and CO_2 combinations, with the π-system of the bridge X, as shown in **I** and **II**. The orbital energies

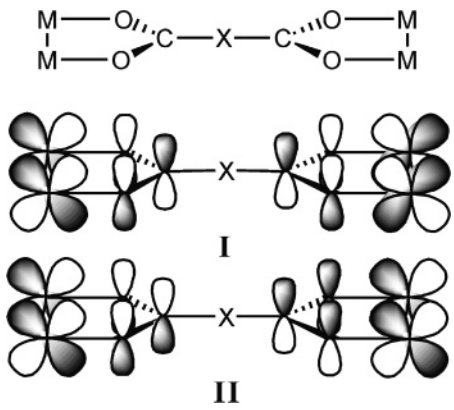

of the two δ combinations are split due to mixing with the π-orbitals of the dicarboxylate bridge, and this leads to a number of interesting properties that are unique to the tetranuclear molecule, as compared to its two single M_2^{4+} centers.

One measure of the degree of electronic coupling that has been commonly investigated is that which is evident from electrochemical studies, typically cyclic voltammetry (CV) and differential-pulsed voltammetry (DPV). In general, these compounds show two reversible oxidation waves and the separation of their potentials is a good guide to the relative degree of electron delocalization in the mixed-valence compounds and the stability of the radical cation with respect to the neutral and doubly oxidized species accordingly to eq 14.[42] A small

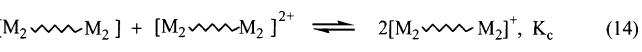

value of K_c, $<10^2$, for example, implies a valence-trapped complex, of class I, in the Robin and Day scheme,[43] whereas a large value of K_c, $>10^6$, almost certainly implies complete delocalization of charge or class III behavior. Values of $K_c \sim 10^3$ imply a strongly coupled system of class II behavior. Various electrochemical data for these compounds are listed in Table 1.

Two important observations can be made from an inspection of Table 1. First, as the distance between the metal centers increases, the degree of electronic coupling falls off. This is particularly well exemplified in the Cotton series of linked Mo_2 complexes employing $O_2C(CH{=}CH)_nCO_2$ bridges, with $n = 1-4$.[35,36] Second, for related pairs of compounds, the electronic coupling is always much greater for tungsten relative to molybdenum. The first effect arises from electron tunneling, which is well-known to fall off with increasing distance, while the second arises from the higher orbital energy of the W_2 δ orbitals. The latter interact more strongly with the π^*-based LUMO of the dicarboxylate bridge.

These compounds are also typically intensely colored as a result of M_2 δ to bridge π^* (MLCT) fully allowed electronic transitions. As a result of the higher orbital energy of the W_2 δ manifold, the electronic absorption spectra of the tungsten complexes are red shifted in comparison to their molybdenum analogues. The splitting of the M_2 δ orbitals and the relative energies of the bridge LUMO are dependent on torsion angles. For example, in the solid state, most oxalate-bridged (OXA) compounds adopt a planar or near-planar structure of the type shown in Figure 7. Calculations on the $(HCO_2)_3Mo_2(\mu\text{-}O_2CCO_2)Mo_2(O_2CH)_3$ model compound employing density functional theory indicate that the planar D_{2h} structure, which is stabilized by M_2 δ to oxalate π^* back-bonding, is only preferred by ca. 5 (M = Mo) to 9 kcal mol^{-1} (M = W) over the fully twisted D_{2d} structure.[30] Thus, in solution we would anticipate that rotations about the central C−C bond would give rise to a Boltzmann's distribution of O−C−C−O torsion angles. It has been suggested that this is the origin of the remarkable thermochromism that these compounds display in 2-methyltetrahydrofuran, 2-MeTHF.[30] See Figure 8.

Many of these dicarboxylate bridged compounds display vibrational features associated with the bridging ligand in their visible absorption spectra.[30,33]

Table 1. Electrochemical Data and Comproportionation Constants for a Series of Dicarboxylate Linked Tetranuclear Compounds

compound	$\Delta E_{1/2}$ (mV)	K_c	ref
$[Mo_2(O_2C^tBu)_3]_2$(oxalate)	280	5.4×10^4	26
$[W_2(O_2C^tBu)_3]_2$(oxalate)	717	1.3×10^{12}	26
$[Mo_2(O_2C^tBu)_3]_2$(tetrafluoroterephthalate)	65	13	26
$[W_2(O_2C^tBu)_3]_2$(tetrafluoroterephthalate)	285	6.6×10^4	26
$[W_2(O_2C^tBu)_3]_2$(1,1′-ferrocenedicarboxylate)	93	37	26
$[Mo_2(O_2C^tBu)_3]_2$(2,3-dioxyquinoxaline)	391	4.1×10^6	26
$[Mo_2(O_2C^tBu)_3]_2$(9,10-dihydroanthracene-1,8-dicarboxylate)	106	62	26
$[W_2(O_2C^tBu)_3]_2$(9,10-dihydroanthracene-1,8-dicarboxylate)	146	2.9×10^2	26
$[W_2(O_2C^tBu)_3]_2$(anthracene-1,8-dicarboxylate)	156	4.3×10^2	26
$[Mo_2(O_2C^tBu)_3]_2$(2,7-dioxynaphthyridine)	389	3.8×10^6	26
$[Mo_2(O_2C^tBu)_3]_2$(anthracene-9,10-dicarboxylate)	60	10	32
$[W_2(O_2C^tBu)_3]_2$(anthracene-9,10-dicarboxylate)	90	33	32
$[Mo_2(O_2C^tBu)_3]_2$(thienyl-2,5-dicarboxylate)	110	72	34
$[W_2(O_2C^tBu)_3]_2$(thienyl-2,5-dicarboxylate)	310	1.7×10^5	34
$[Mo_2(DAniF)_3]_2$(oxalate)	223	5.9×10^3	38
$[Mo_2(DAniF)_3]_2$(acetylenedicarboxylate)	150	3.4×10^2	38
$[Mo_2(DAniF)_3]_2$(fumarate)	137	2.1×10^2	38
$[Mo_2(DAniF)_3]_2$(tetrafluoroterephthalate)	87	30	38
$[Mo_2(DAniF)_3]_2$(carboranedicarboxylate)	69	15	38
$[Mo_2(DAniF)_3]_2$(ferrocenedicarboxylate)	75	19	38
$[Mo_2(DAniF)_3]_2$(malonate)	108	67	38
$[Mo_2(DAniF)_3]_2$(succinate)	100	49	38
$[Mo_2(DAniF)_3]_2$(propane-1,3-dicarboxylate)	112	78	38
$[Mo_2(DAniF)_3]_2$(tetrafluorosuccinate)	121	1.1×10^2	38
$[Mo_2(DAniF)_3]_2$(bicycle[1.1.1]pentane-1,3-dicarboxylate)	95	40	38
$[Mo_2(DAniF)_3]_2$(*trans*-1,4-cyclohexane-dicarboxylate)	69	15	38
$[Mo_2(DAniF)_3]_2$(maleate)	172	3.8×10^3	35
$[Mo_2(DAniF)_3]_2$(allene-1,3-dicarboxylate)	130	1.6×10^2	35
$[Mo_2(DAniF)_3]_2$(*cis*,*cis*-muconate)	125	1.3×10^2	35
$[Mo_2(DAniF)_3]_2$(*trans*,*trans*-muconate)	105	60	35
$[Mo_2(DAniF)_3]_2$(tamuate)	75	19	35
$[Mo_2(DAniF)_3]_2$(texate)	65	13	35
$[Mo_2(DAniF)_3]_2$(terephthalate)	100	49	35

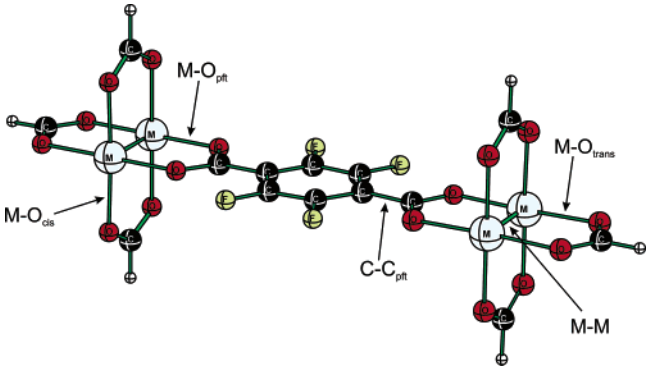

Figure 7. Calculated minimum energy geometry of the D_{2h}-symmetrical $(HCO_2)_3M_2(\mu\text{-OXA})M_2(O_2CH)_3$ complex, where M = Mo or W.[30] The geometry optimization was performed with Gaussian 98, employing D_{2h} symmetry restraints.

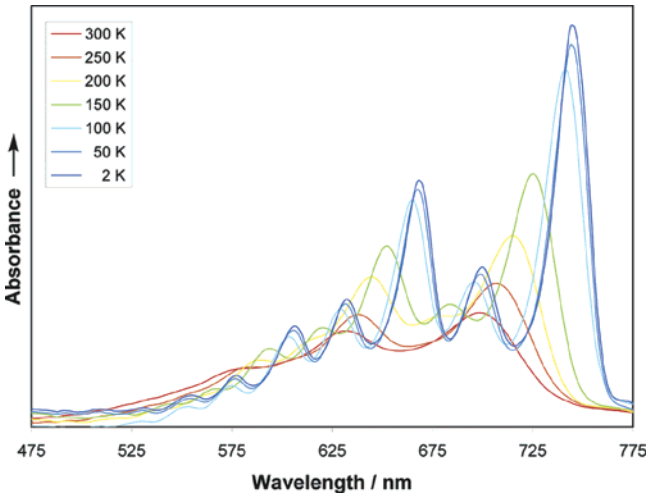

Figure 8. Visible electronic absorption spectra of the $[(^t BuCO_2)_3W_2]_2(OXA)$ compound at 2, 50, 100, 150, 200, 250, and 300 K in 2-MeTHF glass or solution.[30]

These are more pronounced at low temperatures and can be understood in terms of the nature of the MLCT transition that places an electron in an antibonding π^* orbital of the bridge. The low-temperature visible spectrum of the complex $[(^t BuCO_2)_3W_2]_2(\mu\text{-}O_2CCO_2)$ in 2-MeTHF together with its oxalate ^{13}C-labeled isotopomer $(\mu\text{-}O_2{}^{13}C{}^{13}CO_2)$ is shown in Figure 9.[30] There are two progressions in oxalate, ν_1 and ν_2, with the former showing an ca. 50 cm^{-1} isotope shift upon substitution of ^{13}C for ^{12}C. Upon excitation into this MLCT band, these complexes also show very pronounced resonance enhancement of Raman bands associated with the totally symmetric stretching vibrations of the bridge.[30,33]

EPR spectroscopy has also proved to be an invaluable technique for studying electron delocalization in the oxidized radical cations $[(^t BuCO_2)_3M_2]_2(\mu\text{-}O_2C{-}X{-}CO_2)^+$ which are formed by oxidation with $Cp_2Fe^+PF_6^-$ in CH_2Cl_2/THF solvent mixtures.[44] Both molybdenum and tungsten have spin-active nuclei. ^{95}Mo and ^{97}Mo have $I = 5/2$, a similar magnetic moment, and a combined abundance of 25% and for tungsten; ^{183}W has $I = 1/2$ and has 14.5% natural abundance. Both the magnitude and the relative

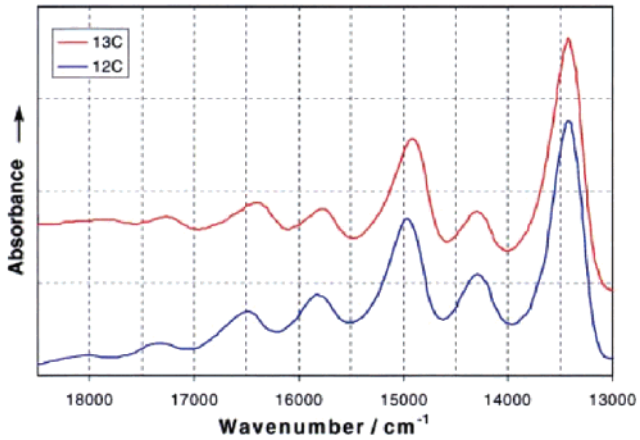

Figure 9. Electronic spectra of $[(^t BuCO_2)_3W_2]_2(OXA)$ and $[(^t Bu^{13}CO_2)_3W_2]_2(oxa)$ at 2 K in a glass of 2-MeTHF.[30]

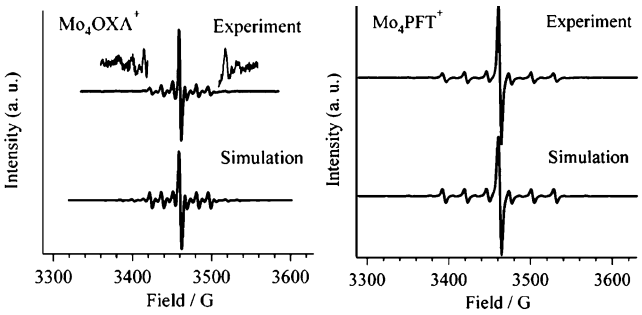

Figure 10. Experimental and simulated electron paramagnetic resonance spectra of $\{[(^t BuCO_2)_3Mo_2]_2(OXA)\}^+$ and $\{[(^t BuCO_2)_3Mo_2]_2(PFT)\}^+$.

intensity of the satellite spectra reflect the degree of electron delocalization, as shown in Figure 10 for the Mo_4-containing radical cations with oxalate and perfluoroterephthalate (PFT) bridges. These correspond to fully delocalized and valence-trapped species, respectively. In general, for a related pair of compounds, the tungsten compound shows the delocalized EPR spectra for $O_2C{-}X{-}CO_2$ bridges, i.e., where X = C_6H_4,[45] C_6F_4,[44] and 2,5-thienyl.[34] In addition, these radical cations show low energy electronic absorption bands in the near-IR, at ca. 5000 cm^{-1}, arising from electronic transitions between the two δ orbital combinations.

2.2.4. Amidato-Bridged Complexes

Cotton and co-workers have made a series of cyclic polyamidato-bridged dimolybdenum complexes, $[Mo_2^{4+}\text{-bridge-}Mo_2^{4+}]$, supported by formamidinate ligands.[46] These bridges are shown in Scheme 1 in the drawings **A**−**H**, where the stereocorrespondence with oxalate is readily apparent. The deprotonated form of these bridging ligands imposes a planar geometry for the Mo_2 atoms. The electrochemical data for these complexes shown in Table 2 reveal that these O,N-bridging ligands are much better at providing electron delocalization in the radical cations than dicarboxylates.

A related O,N-containing ligand, 3,6-dioxypyradizine (DOP) **E** in Scheme 1, was shown by Chish-

Scheme 1

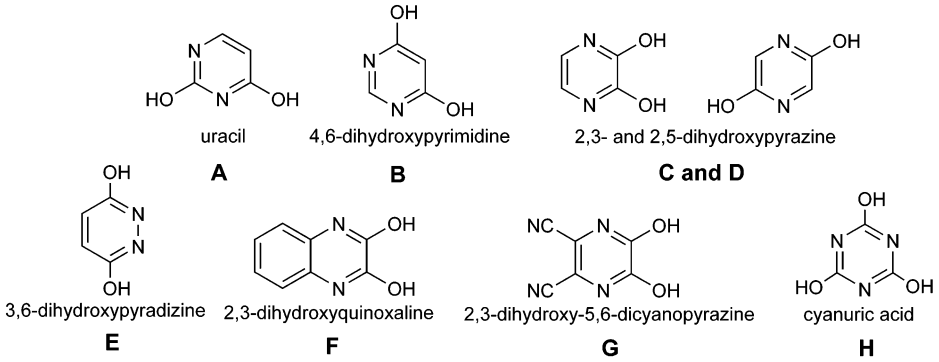

Table 2. Electrochemical Data and Comproportionation Constants for a Series of Polyamido Oxamidate Linked Tetranuclear Compounds

compound	$\Delta E_{1/2}$ (mV)	K_c	ref
$[Mo_2(DAniF)_3]_2$(α-diphenyloxamidate)	191	1.7×10^3	51
$[Mo_2(DAniF)_3]_2$(β-diphenyloxamidate)	540	1.3×10^9	51
$[Mo_2(DAniF)_3]_2$(α-di-*p*-anisyloxamidate)	190	1.6×10^3	51
$[Mo_2(DAniF)_3]_2$(β-di-*p*-anisyloxamidate)	523	6.9×10^8	51
$[Mo_2(DAniF)_3]_2$(μ-4,6-dioxypyrimidinate)	187	1.5×10^3	46
$[Mo_2(DAniF)_3]_2$(μ-2,3-dioxy-1,4-pyrazinate)	258	2.3×10^4	46
$[Mo_2(DAniF)_3]_2$(μ-2,3-dioxyquinoxalinate)	308	1.6×10^5	46
$[Mo_2(DAniF)_3]_2$(μ-2,3-dicyano-5,6-dioxypyrazinate)	263	2.8×10^4	46
$[Mo_2(DAniF)_3]_2$(μ-cyanurate)	152	3.7×10^2	46
$[Mo_2(O_2C^tBu)_3]_2$(μ-3,6-dioxypyradizine)	630	4.5×10^{10}	49
$[W_2(O_2C^tBu)_3]_2$(μ-3,6-dioxypyradizine)	427	1.7×10^7	48

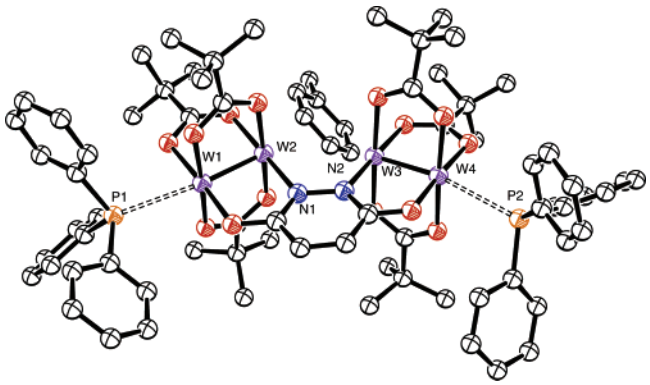

Figure 11. Molecular structure of $\{[W_2(O_2C^tBu)_3]_2(\mu\text{-DOP})\}(PPh_3)_2$·toluene. Hydrogen atoms have been omitted for clarity, and the core P−W−W−N−N−W−W−P arrangement is highlighted.

olm and co-workers[47−49] to link two $M_2(O_2C^tBu)_3$ centers in a somewhat different geometry where the central M···M distances were ca. 3.4 Å. See Figure 11. The electrochemical data for these two compounds (M = Mo and W) are also listed in Table 2 and show that, whereas the molybdenum complex radical cation is much more strongly delocalized than its oxalate counterpart, the tungsten complex is not. On the basis of DFT calculations, it was suggested that the greater delocalization in these O,N-bridged complexes (relative to oxalate) arises from a significant contribution of the bridge π orbitals in the former that provide for a hole-hopping mechanism that is not possible for oxalate.

Cotton and co-workers have also made oxamidate- and *N*,*N*′-diarylterephthaloyldiamidate-bridged Mo_2^{4+}-containing complexes supported by formamidinate ligands.[50] These are analogues of oxalate- and terephthalate-bridged compounds. Of particular note was the isolation of two isomers of the oxamidate-bridged compounds.[51] The so-called α isomer forms five-membered rings, as does oxalate in binding to the dimetal center, but for steric reasons, the Mo_2 units are perpendicular to one another. In the β isomer, there are six-membered rings involving the Mo_2 units and the whole central moiety is planar. These bridging motifs are shown in drawings **III** and **IV**. The

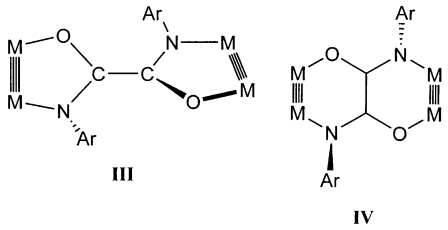

electrochemical studies revealed that the electronic coupling in these two isomers was dramatically different, as evidence by $K_c \sim 10^3$ for the α isomer and $K_c \sim 10^9$ for the β isomer. The difference is understandable in terms of M_2 δ-to-bridge π-conjugation, which is maximized for the planar β isomer.

2.2.5. EX_4^{2-} Bridges

Cotton and co-workers have made a series of compounds of the form $[(formamidinate)_3Mo_2]_2(\mu\text{-}X_2EX_2)$, where X_2EX_2 is SO_4^{2-},[52] MoO_4^{2-},[52] WO_4^{2-},[52] $Zn(OMe)_4^{2-}$,[53] and $Co(OMe)_4^{2-}$.[53] In all of these, the two M_2 units are perpendicular but brought into close proximity. Despite the close proximity, the electrochemical behavior of these complexes with K_c values $\sim 10^3$ implies class II-like behavior. Furthermore, chemical oxidation of the complexes having $M(OMe)_4^{2-}$ bridges where M = Zn or Co yielded salts that were crystallographically characterized and shown to have fully localized or valence-trapped ions on the basis of Mo−Mo distances of 2.151(1) and 2.116(1) Å for M = Zn, corresponding to bond orders of 3.5 and 4, respectively.[54] Similar Mo−Mo distances were observed for M = Co. The valence-trapped nature of these Mo_4-containing cations was also evident from EPR spectroscopy.

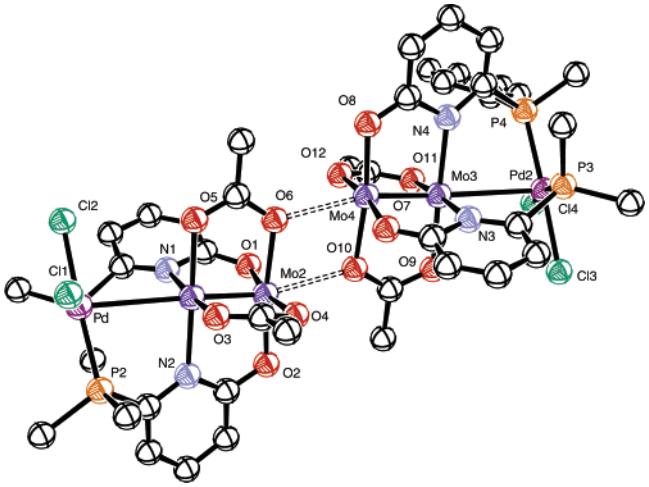

Figure 12. Molecular structure of $[Mo_2PdCl_2(pyphos)_2(OAc)_2]_2$, wherein the diagonal acetate oxygen to axial Mo interaction is illustrated with dashed bonds. Hydrogen atoms and pyphos phenyl rings omitted for clarity.

2.2.6. Oxygen Donor Bridges of Molybdenum

The complex $[Mo_2PdCl_2(pyphos)_2(OAc)_2]_2$ (pyphos = 6-(diphenylphosphino)-2-pyridonate) was obtained in 5% yield by treating $PdCl_2(pyphosH)_2$ with sodium hydroxide and reacting it with a 1:1 mixture of $Mo_2(OAc)_4$ and $[Mo_2(OAc)_2(CH_3CN)_6]^{2+}$.[55] The Pd−Mo distances suggest that there is no interaction between the two metal atoms. The Mo−Mo distances are consistent with a quadruple bond description. The two Mo_2 units interact with an O atom of a μ-acetate ligand on the neighboring Mo_2 unit to form a dimeric structure, shown in Figure 12.

The platinum analogues of this complex can also be prepared by using similar reaction conditions and $PtX_2(pyphosH)$, X = Cl, Br, I, starting materials. The $[Mo_2PtX_2(pyphos)_2(OAc)_2]_2$ complexes were obtained by reacting $PtX_2(pyphosH)_2$ with a 1:1 mixture of $Mo_2(OAc)_4$ and $[Mo_2(OAc)_2(CH_3CN)_6]^{2+}$.[56] The reaction between $[Mo_2(O_2C^tBu)_2(CH_3CN)_4]^{2+}$ and $PtX_2(pyphosH)_2$ gave the corresponding pivalato complexes, $[Mo_2PtX_2(pyphos)_2(O_2C^tBu)_2]_2$.[56] In these complexes, one of the axial sites of the Mo−Mo quadruply bonded core is occupied by a platinum atom; hence, the three metal atoms are aligned linearly. The two mutually *cis* pyphos ligands coordinate the platinum atom through their P atoms and bridge the Mo_2 center with their N and O atoms. The Mo_2 core is also bridged by two mutually *cis* carboxylate ligands. The Mo−Mo distances are comparable to those found in $Mo_2(pyphos)_4$ and $Mo_2(OAc)_4$. The Pt−Mo distances indicate that bonding between the Mo_2 unit and Pt is weak. The dimeric structure of the complexes is due to the fact that the O atom of the pyphos ligands is situated in close proximity to the Mo atom on the neighboring molecule. It is noteworthy that the geometry of the axial Mo···O interaction is different from that in the palladium complex where the O atom of the bridging carboxylate ligand interacts with the adjacent Mo_2 core to form a dimeric structure. The bonding in the palladium complex is similar to that which is usually found in the infinite structures of the dimolybdenum tetrakis(μ-carboxylato) complexes.

Another example of the formation of a dimer of "dimers" linked by the relatively weak axial Mo···O interactions is $[Mo_2(mhp)_3(CH_3CN)_2][BF_4]$ (mhp = 2-hydroxy-6-methylpyridinate).[57] The complex was prepared by treating $Mo_2(mhp)_4$ with 1 equiv of Et_3OBF_4 in acetonitrile. The cationic portion crystallizes as a weakly associated dimer of Mo_2^+ units. The axial position of each Mo−Mo bond is protected by two mhp methyl substituents on one end and only one mhp methyl on the other, which allows the dimerization to occur via axial Mo···O interactions. This situation is in direct contrast to that of carboxylate-supported cations such as $[Mo_2(O_2C^tBu)_2(CH_3CN)_6][BF_4]_2$, which satisfy their axial sites with acetonitrile.

2.2.7. Rhenium Complexes

There have been far fewer reports of dimers of "dimers" containing rhenium than there have been for molybdenum and tungsten. The first reported rhenium-containing dimer of "dimers" was $(^nBu_4N)_2[[Re_2Cl_7]_2\{\mu\text{-PP}\}]$ (PP = $Ph_2PC{\equiv}CPPh_2$ (dpa) or *trans*-$Ph_2PCH{=}CHPPh_2$) (dppee)), prepared by reacting $(^nBu_4N)_2Re_2Cl_8$ and the diphosphine in a methanol/HCl mixture.[58] Both of the dimers of "dimers" have been characterized by ^1H NMR spectroscopy; however, neither product was characterized crystallographically. The resulting dimers of "dimers" were only slightly soluble but were shown to react with monodentate phosphines to produce dinuclear species.[58] The dpa-bridged dimer of "dimers" was shown to react with PEt_3 to form $Re_2Cl_4(PEt_3)_4$ while $Re_2Cl_5(PMePh_2)_3$ and $Re_2Cl_5(PEtPh_2)_3$ formed upon the reaction with $PMePh_2$ and $PEtPh_2$, respectively.[58] The dppee-linked dimer of "dimers" displays similar reactivity toward monodentate phosphines.[58] The products obtained in these reactions are identical to those expected from such a Re_2^{6+} quadruply bonded starting material.[3] The cyclic voltammagram of the dpa-linked species contained two closely spaced redox couples, −0.31 V and −0.43 V vs Ag/AgCl, which signify the reductions of the two Re_2^{6+} cores occur at different potentials. A similar $\Delta E_{1/2}$ was observed for the dppee species.[58]

A rhenium-containing dimer of "dimers" linked by oxygen and hydroxy ligands, $[Re_4(C_6H_5NCOCH_3)_6Cl(\mu\text{-O})(\mu\text{-OH})(MeOH)_3][ReO_4]_2$,[59] was prepared by reacting $Re_2(C_6H_5NCOCH_3)_4Cl_2$ with air and moisture. The cationic portion of the compound is a tetranuclear species that contains two quadruply bonded Re_2 units linked by oxygen and hydroxy ligands to form a five-membered ring containing three Re atoms.

Cotton and co-workers prepared a dimer of "dimers" that contained highly unsymmetrical Re−Re bonds linked by two oxo bridges, $[Cl(PMe_3)_3Re(\mu\text{-}O_2CC_6H_5)Re(O)]_2(\mu\text{-O})_2$, by reacting $Re_2(O_2CC_6H_5)_4Cl_2$ and PMe_3 in ethanol with subsequent addition of H_2O_2.[60] At the center of the tetranuclear molecule is a rhombic $Re_2(\mu\text{-O})_2$ unit in which each oxo-bridge is unsymmetrical. The Re···Re distance across this rhombus is 3.007 Å, which indicates the absence of significant direct Re···Re bonding. The overall oxidation number of each Re_2 unit is +6; however, on the basis of the

Re−Re bond distance of 2.3396(8) Å, the Re_2 units do not contain a homopolar Re−Re quadruple bond. The oxidation states of the Re atoms within the dinuclear unit can be estimated as being between +1/+5 and +2/+4.

The dimer of "dimers" [*cis*-$Re_2(\mu\text{-}O_2CCH_3)_2Cl_4(pyz)]_2(\mu$-pyz) was obtained by slow diffusion of an excess of pyrazine in acetone into an aqueous solution of *cis*-$Re_2(O_2CCH_3)_2Cl_4(H_2O)_2$.[61] The Re−Re distance of 2.240 Å is consistent with the presence of a Re−Re quadruple bond. If a 1:1 stoichiometry of pyrazine and *cis*-$Re_2(O_2CCH_3)_2Cl_4(H_2O)_2$ is used, a polymer is formed, vide infra.

2.3. Loops, Cyclotrimers, Cyclotetramers, and Polygons

Dicarboxylate bridges having methylene units, such as in $O_2C(CH_2)_nCO_2$ (n = 2−8)[62] and in malonate,[63] have been employed in the synthesis of compounds that have become known as molecular loops. See Figure 13. These aliphatic bridges impede electronic communication between the two MM quadruple bonds, as judged by electrochemical measurements.[63] Cotton and co-workers have prepared an enantiomerically pure chiral loop by reacting *cis*-$[Mo_2(DAniF)_2(NCMe)_4](BF_4)_2$ with a chiral dicarboxylate which was prepared from hydroquinone and ethyl (*S*)-lactate.[64]

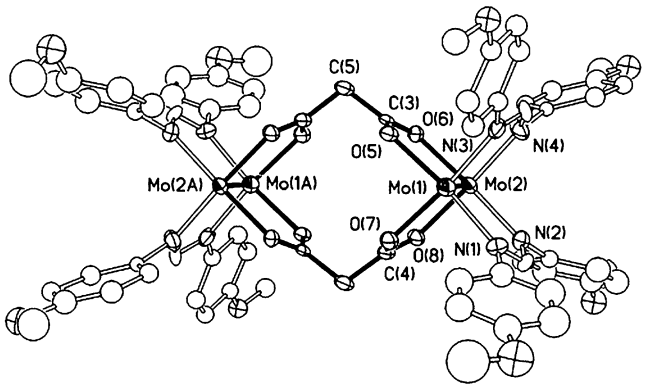

Figure 13. Molecular structure of $[Mo_2(DAniF)_2]_2(\mu\text{-}O_2CCH_2CO_2)_2$. Hydrogen atoms, except for those on the bridging methylene group, are omitted for clarity. The DAniF anisole groups are also omitted for clarity.[63]

The reactions involving a large number of dicarboxylate anions with $Mo_2(form)_2(CH_3CN)_4^{2+}$ salts have been shown to yield cyclotetramers,[65,66] $[Mo_2(form)_2(O_2CXCO_2)]_4$, as summarized in Scheme 2. The molecular structures of the oxalate[65] and the 1,1′-ferrocenylcarboxylate compounds[65] are shown in Figures 14 and 15, respectively.

The redox chemistry of the oxalate-bridged complex shows three reversible oxidation waves, implying that there is extensive electronic coupling between the four Mo_2^{4+} centers.[65] Electronic structure calculations employing density functional theory (DFT) have been performed on the model compounds $[(HCO_2)_2Mo_2(O_2CCO_2)]_4$ in D_{4h} symmetry and have indicated a significant splitting between the Mo_4 δ orbitals because of coupling through the oxalate π-system.[29,31] The frontier molecular orbitals are shown in Figure 17, and the calculated energy level diagram is shown in Figure 16. With the more flexible linker, 1,4-cyclohexanedicarboxylate, and $Mo_2(form)_2(CH_3CN)_4^{2+}$, a cyclotrimer, $[Mo_2(form)_2(O_2CC_6H_{10}CO_2)]_3$, was formed.[67] The molecular structure of this compound is shown in Figure 18.

Scheme 2

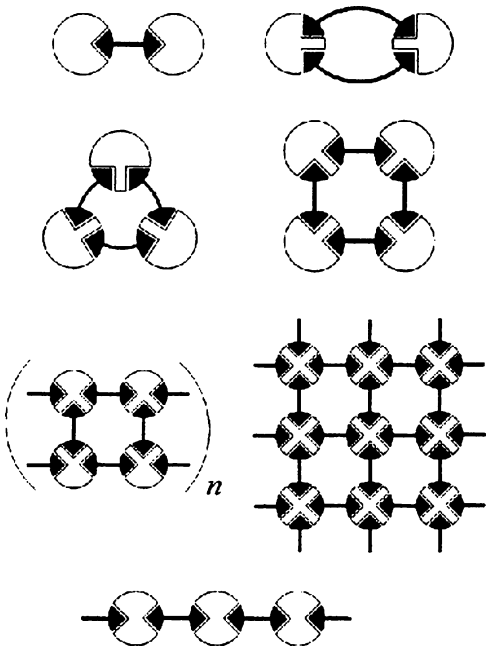

Often these compounds are referred to as molecular triangles and squares, and related rhodium compounds have also been extensively studied by the Cotton group, who have shown, in at least certain cases, that the cyclotrimers and cyclotetramers are present in solution in equilibrium.[65−67] The Cotton group has also shown that, for Rh_2^{4+} units, "loops, triangles and squares" can be used to form supramolecular coordination polymers in the solid state by

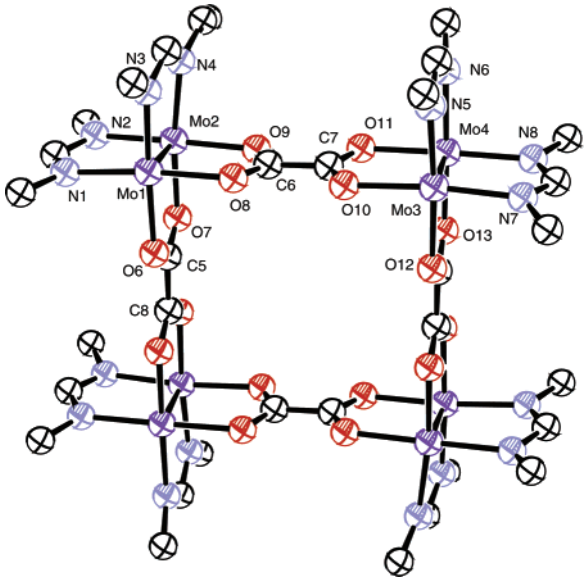

Figure 14. Molecular structure of the $[(form)_2Mo_2(oxalate)]_4$ square complex. Cocrystallized solvent molecules, hydrogen atoms, and formamidinate OMe groups are omitted for clarity. Only one set of symmetry equivalent atoms is labeled.

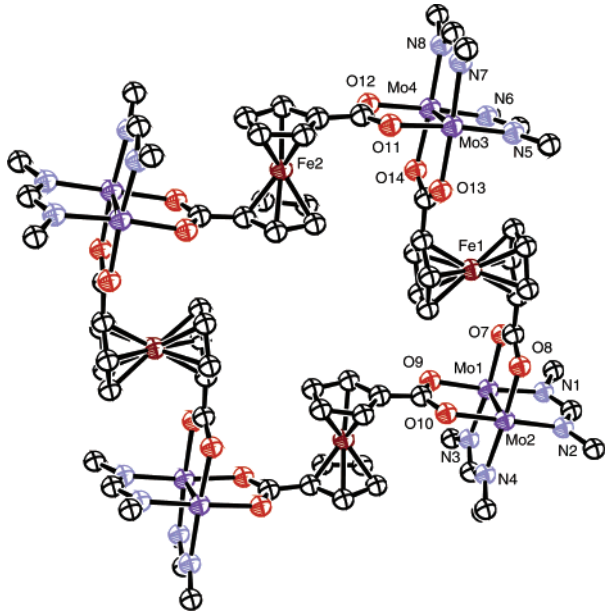

Figure 15. Molecular structure of the $[(form)_2Mo_2(\text{-}Cp\text{-}Fe\text{-}Cp\text{-})]_4$ square complex. Cocrystallized solvent molecules, hydrogen atoms, and formamidinate OMe groups are removed for clarity. Only one set of symmetry equivalent atoms is labeled.

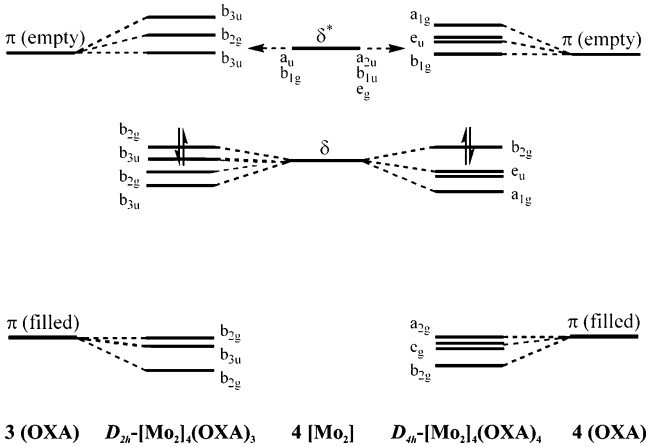

Figure 16. Frontier molecular orbital diagram for the $[(HCO_2)_2Mo_2(OXA)]_4$ square complex. The electronic structure of the square was calculated using Gaussian 98 with D_{4h} symmetry restraints.

use of axial linkers such as 4,4′-bipyridine which bind along the M−M axis.[68] However, these have not yet been seen for Mo_2^{4+}-containing compounds, presumably due to weaker axial ligation to the Mo_2^{4+} units.

Cotton also has prepared a higher order polygon derived from the anion of trimesic acid and $Mo_2(form)_2(CH_3CN)_4^{2+}$.[69,70] A similar compound of rhodium has also been made with a stoichiometry of $[M_2(cis\text{-}DAniF)_2]_6(1,3,5\text{-}C_6H_3(CO_2)_3)_4$.[70] The central unit of the molybdenum-containing polygon is shown in Figure 19. The carbonate dianion has also been employed as a linker and shown to be capable of generating triangles[71] and squares.[72]

The formations of these molecular loops, triangles, squares, and the polygon noted above all arise from the *cis*-templating influence of the $Mo_2(form)_2^{2+}$ unit when the other attendant ligands have a weaker *trans*-influence, e.g., as seen for CH_3CN and oxygen donors.

2.4. Extended Chains

2.4.1. Shorter Chains

Chains containing Cr−Cr quadruple bonds have been prepared in which a linear array of metal atoms are surrounded by four chain ligands that serve to keep adjacent metal ions within bonding distance of each other. The reaction of the lithium salt of bis(2-pyridyl)formamidinate (DpyF) with $CrCl_2$ results in the production of a mixture of $[Cr_3(DpyF)_4][PF_6]_2$ and $[Cr_4(DpyF)_4Cl_2]Cl_2$, both of which have been structurally characterized.[73] In the $[Cr_4(DpyF)_4Cl_2]Cl_2$ complex, the difference between the central and outer Cr−Cr distances is very large, ca. 2.73 Å vs ca. 2.01 Å. The bonding in the complex can be described as consisting of two Cr−Cr quadruple bonds and little or no bonding between the two inner chromium atoms. The reaction of $CrCl_2$ with the dilithium salt of tripyridyldiamine (tpda) yielded $Cr_5(tpda)_4Cl_2\cdot CH_2Cl_2$.[74] The Cr−Cr distances along the essentially linear chain correspond to Cl−Cr···Cr^{-4}−Cr···Cr^{-4}−Cr−Cl. As expected, the polypyridyldiamido ligands form a spiral around the core of metal atoms.

The treatment of $Mo_2(O_2CCHF_2)_4$, prepared from $Mo_2(OAc)_4$ by ligand exchange, with 2 equiv of Et_3OBF_4 in a CH_2Cl_2/CH_3CN mixture resulted in the production of $[Mo_2(O_2CCHF_2)_2(CH_3CN)_4][BF_4]_2$. The complex $[Mo_2(O_2CCHF_2)_2(bpy)_2(CH_3CN)(BF_4)][BF_4]$ was prepared by reacting $[Mo_2(O_2CCHF_2)_2(CH_3CN)_4][BF_4]_2$ with 2 equiv of bpy. The combination of $Mo_2(O_2CCHF_2)_4$, $[Mo_2(O_2CCHF_2)_2(bpy)_2(CH_3CN)(BF_4)][BF_4]$, and $CHF_2CO_2^-$ in a 1:2:4 mole ratio yielded $[Mo_6(O_2CHF_2)_{12}(bpy)_4]$.[75] This product reflects the reaction stoichiometry, in that a central $Mo_2(O_2CCHF_2)_4$ unit is linked to two $[Mo_2(O_2CCHF_2)_2(bpy)_2]^{2+}$ units by two bridging $CHF_2CO_2^-$ groups and, therefore, can be conveniently, if not entirely accurately, described as a trimer of "dimers".

2.4.2. Dimolybdenum Building Blocks

The first examples of the incorporation of quadruply bonded metal−metal complexes into low-dimensional polymeric arrays were prepared by making use of the empty coordination sites in the axial positions of M_2L_8-type compounds. The major drawback of materials prepared using this strategy is that the M−L axial bonds are relatively weak and substitutionally labile, owing to the strong *trans* influence and *trans* effect exerted by the metal−metal multiple bond. As a result, the integrity of polymers of this type is jeopardized by the relatively weak $M-L_{ax}-M$ backbone. In fact, these polymers only exist in the solid state and are not present in solution.

Linear chain compounds were obtained upon the reaction of $Mo_2(OAc)_4$ with an excess of the bidentate ligands pyrazine, 4,4′-bipyridine, and dabco (1,4-diazabicyclo[2.2.2]octane).[76,77] All compounds were found to have a $Mo_2(OAc)_4$:L stoichiometry of 1:1. The L = bpy species was characterized by X-ray crystallography. The structure, shown in Figure 20, consists of alternating $Mo_2(OAc)_4$ and bpy units in a nearly linear chain.[76] The other compounds in the series are presumed to also have linear structures. The reaction

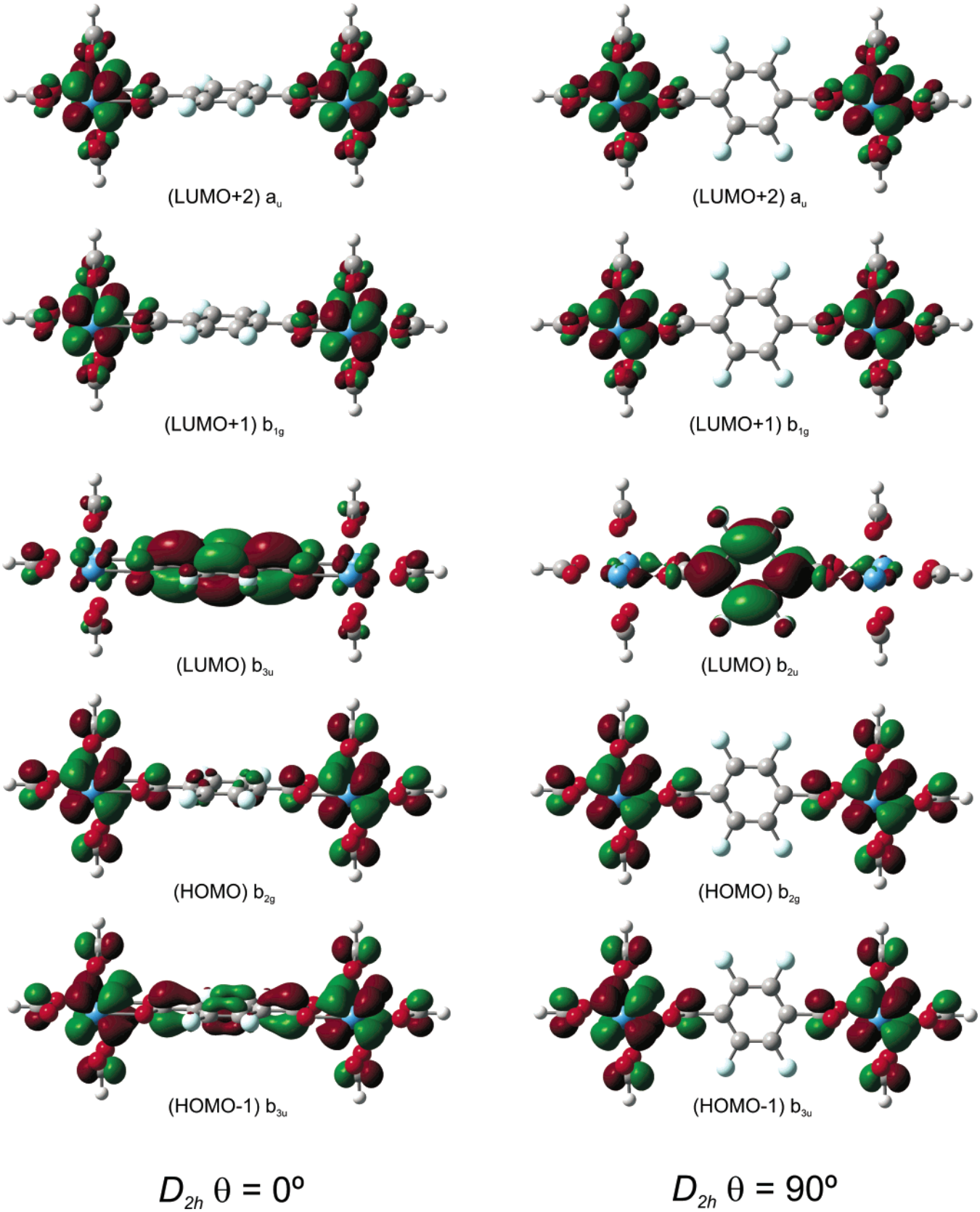

Figure 17. Calculated molecular orbital diagrams for the $[(HCO_2)_3Mo_2]_2(O_2C-C_6H_4-CO_2)$ complex having the phenyl ring oriented parallel to the MM axes (left) and perpendicular to the MM axes (right). The electronic structure of this complex was calculated using Gaussian 98® with D_{2h} symmetry restraints.

of $Mo_2(O_2C^tBu)_4$ with 2 equiv of bpy yielded the 1:1 complex $[Mo_2(O_2C^tBu)_4(bpy)]_n$.[78] The Mo−N distances along this chain, 2.665 and 2.679 Å, indicate that the bpy ligand is weakly coordinated. The Mo−Mo distances, 2.092 and 2.099 Å, are slightly longer than the Mo−Mo distance in the parent complex.

A very different structure was obtained when $Mo_2(O_2CCF_3)_4$ was treated with 4,4′-bipyridine under

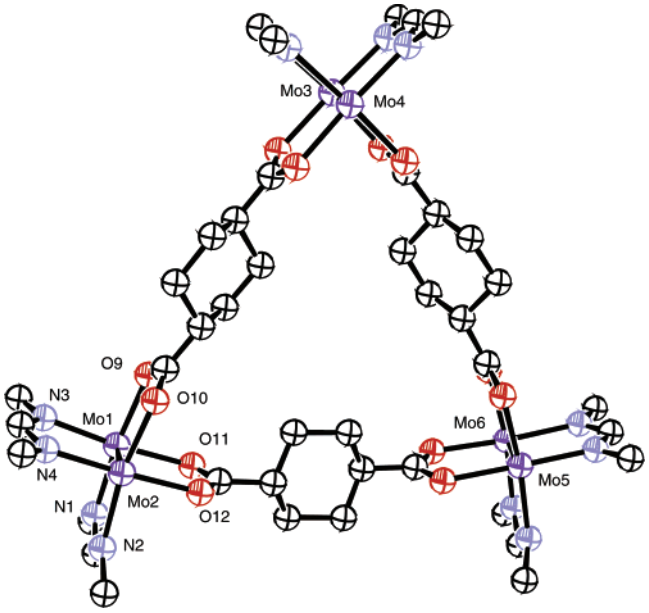

Figure 18. Molecular structure of the $[(form)_2Mo_2(O_2C-c\text{-}C_6H_{10}-CO_2)]_3$ triangle complex. Cocrystallized solvent molecules, hydrogen atoms, and formamidinate OMe groups are removed for clarity. All of the molybdenum atoms and one set of ligand N and O atoms have been labeled.

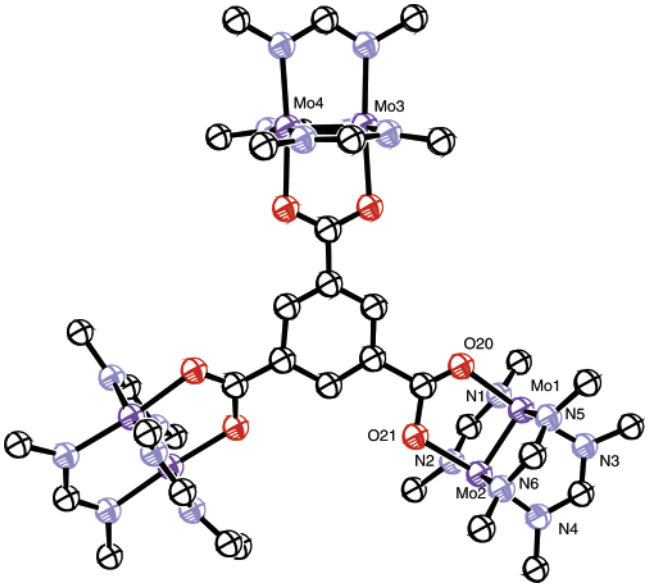

Figure 19. Molecular structure of the $[(form)_3Mo_2]_3[C_6H_3(CO_2)_3]$ complex. Cocrystallized solvent molecules, hydrogen atoms, and formamidinate OMe groups are removed for clarity.

reaction conditions similar to those used to prepare the $Mo_2(OAc)_4$- and $Mo_2(O_2C^tBu)_4$-based chains. The product of this reaction has a $Mo_2(O_2CCF_3)_4$:bpy stoichiometry of 3:4. X-ray structural analysis of $(Mo_2(O_2CCF_3)_4)_3\cdot(bpy)_4$ revealed that the crystal consists of polymer chains formulated as $[Mo_2(O_2CCF_3)_4\cdot(bpy)]_n$ and discrete bis bpy adduct dimers, $Mo_2(O_2CCF_3)_4\cdot(bpy)_2$.[79] The discrete dinuclear complexes are located between the infinite chains of $[Mo_2(O_2CCF_3)_4\cdot(bpy)]_n$, which are made up of alternating $Mo_2(O_2CF_3)_4$ and bpy units and are essentially linear. The coexistence of polymer chains and discrete dinuclear complexes in the same crystal is unprecedented. In general, axial coordination is stronger in

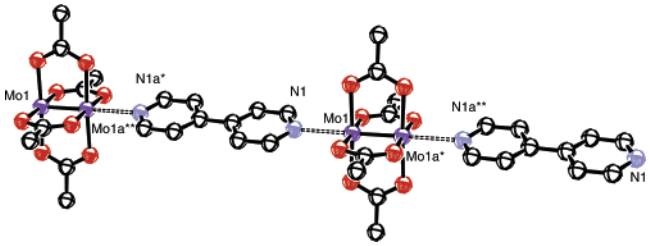

Figure 20. Molecular structure of the polymeric $Mo_2(OAc)_4$-(bpy). The bpy to Mo interaction has been illustrated with a dashed bond. Hydrogen atoms have been removed for clarity. The molybdenum and bpy nitrogen atoms are labeled.

$Mo_2(O_2CCF_3)_4$-containing species than in $Mo_2(OAc)_4$-containing species; as a result the Mo−N distances in $Mo_2(O_2CCF_3)_4$ complexes are 0.06−0.2 Å shorter than those in $Mo_2(OAc)_4$ complexes. This shortening of the Mo−N bonds may be due to the presence of electron-withdrawing CF_3 groups on the carboxylate ligands, which enhance the Lewis acidity of the metals and lead to the strengthening of the metal−ligand bonds.

The reaction of $Mo_2(O_2CCF_3)_4$ with 1 equiv of a *p*-quinone produced a series of chain complexes with the formula $[Mo_2(O_2CCF_3)_4\cdot(p\text{-quin})]_n$ (*p*-quin = 9,10-anthraquinone (AQ), 2,6-dimethyl-1,4-benzoquinone, and 1,4-naphthoquinone).[80] X-ray structural analysis of these complexes showed that the carbonyl oxygens of the paraquinone are coordinated to the Mo_2 dinuclear units. The Mo−Mo bond distances 2.107(1)−2.117(1) Å are slightly longer than that of the parent $Mo_2(O_2CCF_3)_4$. Elongation of C=O and C=C bonds was observed for 9,10-anthraquinone and 2,6-dimethyl-1,4-benzoquinone but not for 1,4-naphthoquinone.[80] This can be explained in terms of the relative oxidizing abilities of the *p*-quinones and possibly their symmetries. The $\delta \rightarrow \delta^*$ transition occurs at ~440 nm in the diffuse reflectance spectrum for the three $[Mo_2(O_2CCF_3)_4\cdot(p\text{-quin})]_n$ complexes, which is energetically very similar to the $\delta \rightarrow \delta^*$ transition in the parent complex, 434 nm. The complex $[Mo_2(O_2CCF_3)_4\cdot AQ]_n$ is EPR silent at room temperature. These results suggest that no significant change in electronic structure of the Mo_2 unit occurs upon polymer formation and, therefore, that the expected interaction of $Mo_2(O_2CCF_3)_4$ with the energetically low lying LUMO of AQ does not occur.[81]

Infinite zigzag chains of $Mo_2(OAc)_4$ units, linked by dmpe (dmpe = 1,2-bis(dimethylphosphino)ethane) and methyl-substituted derivatives of ethylenediamine, are obtained by dissolving $Mo_2(OAc)_4$ in the appropriate neat ligand.[82] X-ray quality light yellow crystals of $[Mo_2(OAc)_4(dmpe)]_n$ were obtained in low yield by stirring $Mo_2(OAc)_4$ in hot dmpe for several hours and then cooling the solution to room temperature. EDAX analysis of the crystals found that the Mo:P ratio was 1:1. The $[Mo_2(OAc)_4(dmpe)]_n$ polymer is insoluble in most organic solvents; however, it can be redissolved in neat dmpe. The structure of $[Mo_2(OAc)_4(dmpe)]_n$ comprises an infinite array of $Mo_2(OAc)_4$ units bridged by dmpe. The $Mo_2(OAc)_4$ units in the polymer chain are relatively unperturbed with a Mo−Mo distance, 2.105 Å, which is very close to that of the parent complex, 2.093 Å. The relatively

long Mo−P contacts are characteristic of weak axial interactions. The tetrahedral carbon and phosphorus atoms of the dmpe impart a zigzag geometry.[82]

The $[Mo_2(OAc)_4(tmed)]_n$ (tmed = tetramethylethylenediamine) polymer was prepared by heating $Mo_2(OAc)_4$ in neat tmed. Upon slow cooling of the $Mo_2(OAc)_4$/tmed solution, large, light yellow, single crystals of $[Mo_2(OAc)_4(tmed)]_n$ formed in high yield. The tmed-bridged polymer, like its dmpe analogue, is insoluble in common organic solvents yet can be redissolved in warm tmed.[82] In contrast to the zipzag structure of the dmpe polymer, the tmed ligands yield a linear chain. The one-dimensional polymers $[Mo_2(OAc)_4(N,N'dmed)]_n$ and $[Mo_2(OAc)_4(pda)]_n$ were obtained by dissolving $Mo_2(OAc)_4$ in neat dmed (N,N′dmed = *N*,*N*′-dimethylethylenediamine) and pda (pda = 1,3-diaminopropane), respectively.[83] The structures of these polymers were found to be very similar to those of their dmpe and tmed analogues. Crystalline samples of the $[Mo_2(OAc)_4(diamine)]_n$ polymers thermally decompose, in inert atmospheres, to form crystalline $Mo_2(OAc)_4$ at temperatures less than 120 °C. Thermogravimetric analysis studies carried out on the diamine-bridged polymers revealed that the diamine ligands are expelled at temperatures at or below the boiling points of the pure diamines.[83] The weakness of the bonds joining the Mo_2 and ligand units together in these complexes precludes any one-dimensional properties.

If the diamine used in the reaction is ethylenediamine, *N*,*N*-dmed, or *N*-med, complexes with a very different structure are obtained. These diamines react with $Mo_2(OAc)_4$ upon gentle warming, resulting in the displacement of an acetate ligand from the Mo_2 center. Upon cooling, pale-orange yellow crystals of $\{[Mo_2(OAc)_3(diamine)_2][OAc]\}_2 \cdot x$diamine (diamine = *N*,*N*-dmed, $x = 0$; *N*-med, $x = 1$; en, $x = 1$) formed.[83] In these complexes, each Mo atom possesses a chelating diamine with the $-NH_2$ group bound in the equatorial position previously occupied by the displaced acetate ligand. The two $[Mo_2(OAc)_3(diamine)_2]^+$ units are linked together via hydrogen bonding between the equatorial $-NH_2$ diamine hydrogens and the oxygens of the displaced acetate groups. These results suggest that an $-NH_2$ functionality is necessary in order for acetate displacement to occur. The role of the $-NH_2$ functionality is to stabilize the displaced acetate ions in the solid state through hydrogen bonding.

Another approach that has been used to prepare one-dimensional polymers containing quadruply bonded metal−metal complexes is to use polynitriles to assemble the dinuclear centers into inorganic−organic hybrid structures. The reaction of $Mo_2(O_2CCF_3)_4$ with TCNQ (TCNQ = 7,7,8,8-tetracyanoquinodimethane) in refluxing xylenes resulted in a red solution, which yielded dark red crystals upon cooling. An X-ray crystallographic study revealed that the compound is composed, in part, of a chain of μ_4-TCNQ ligands bound to the axial sites of four independent $Mo_2(O_2CCF_3)_4$ molecules to give a one-dimensional polymer motif.[84] A second type of $Mo_2(O_2CCF_3)_4$ molecule is located in a cavity with two *m*-xylene ligands perpendicularly oriented near the

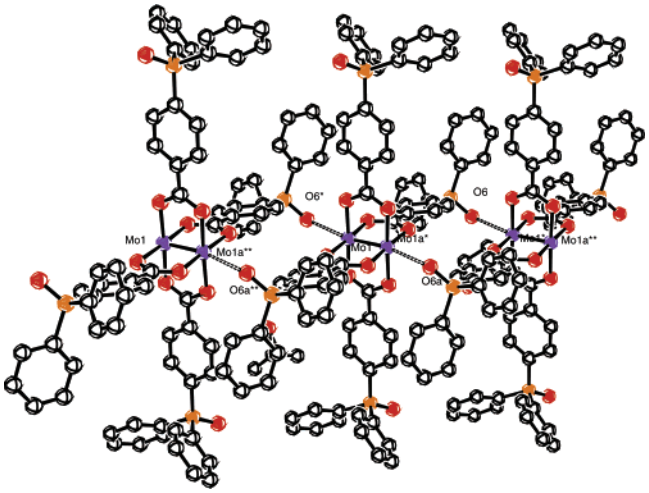

Figure 21. Extended molecular structure of the $Mo_2[O_2CC_6H_4P(O)Ph_2]_4$ complex. The phosphine oxide oxygen to axial Mo interaction is illustrated with a dashed bond. Hydrogen atoms are removed for clarity. The molybdenum and oxygen atoms involved in the intermolecular aggregation are labeled.

axial positions. The Mo−Mo bond length in the polymeric chain, 2.1126 Å, is not statistically different from the Mo−Mo distance in the molecule of $Mo_2(O_2CCF_3)_4(m\text{-xylene})_2$. However, these distances are longer by ca. 0.023 Å than the corresponding Mo−Mo distance in $Mo_2(O_2CCF_3)_4$. The Mo−N(TCNQ) distance of 2.627 Å is longer than the corresponding Mo−N distances for other polymeric $Mo_2(O_2CCF_3)_4L_2$ complexes containing axial nitrogen donor ligands. These observations, taken together with ν(CN) data, imply that the interactions between the Mo_2 unit and the TCNQ are weak σ interactions. The TCNQ is also involved in π-stacking interactions with interstitial *m*-xylenes.

The reaction of $Mo_2(O_2CCF_3)_4$ with DM-DCNQI (DM-DCNQI = 2,5-dimethyl-*N*,*N*′-dicyanoquinone diimine) in benzene results in the instantaneous formation of yellow-brown needles of $[Mo_2(O_2CCF_3)_4(DM\text{-}DCNQI)\cdot C_6H_6]_n$.[85] The increase in the ν(CN) stretch in the polymer relative to the ν(CN) stretch for the free DM-DCNQI and the pale color of the compound are both consistent with the assignment of DM-DCNQI as a neutral ligand. The structure consists of alternating $Mo_2(O_2CCF_3)_4$ and DM-DCNQI molecules, which form a zigzag polymeric chain. The Mo−Mo distance of 2.127 Å and the axial Mo−N distance of 2.531 Å are both in the normal range for molecular $Mo_2(O_2CCF_3)_4$ compounds with axial nitrogen donor ligands. The stability of the compound and the ease with which it crystallizes from benzene were rationalized on the basis of π-stacking of the DM-DCNQI ligands and benzene molecules.[85]

Walton and co-workers have incorporated quadruply bonded dimolybdenum units into a two-dimensional polymeric assembly by using the asymmetric $[4\text{-}Ph_2P(O)C_6H_4CO_2]^-$ ligand as a linker. The reaction of $K_4Mo_2Cl_8$ with $4\text{-}Ph_2P(O)C_6H_4CO_2H$ in refluxing ethanol produced an insoluble compound with the formula $\{Mo_2[\mu\text{-}O_2CC_6H_4\text{-}4\text{-}P(O)PPh_2]_4\cdot 4EtOH\}_n$.[86] The X-ray crystal structure shows that the P=O groups link the individual $[Mo_2(\mu\text{-}O_2CC_6H_4P(O)Ph_2)_4]$ units

into a two-dimensional polymeric array, as shown in Figure 21.

2.4.3. Dichromium Building Blocks

Another example of a linear chain with a 1:1 M_2:L stoichiometry is $Cr_2(OAc)_4$·pyrazine, which is formed by treating $Cr_2(OAc)_4$ with 1 equiv of pyrazine. The bifunctional pyrazine ligand links the dichromium units into a slightly zigzagged chain.[87] Crystallographic centers of inversion are located at the midpoints of the Cr−Cr bonds and at the centers of the pyrazine ligands. The Cr−Cr distance of 2.295 Å is surprisingly short; in fact, it is among the shortest reported for a dichromium carboxylate-bridged complex. The pyridine and piperidine adducts of $Cr_2(OAc)_4$ have longer Cr−Cr distances, which is consistent with the greater basicity of these ligands as compared to pyrazine.

2.4.4. Dirhenium Building Blocks

A series of one-dimensional polymers containing quadruply bonded dirhenium units was prepared by taking advantage of the substitutional lability of the axial water ligands in the complex *cis*-$Re_2(O_2CCH_3)_2Cl_4(H_2O)_2$. Three bidentate ligands, pyrazine, 4,4′-bipyridine, and methylenebis(diphenylphosphine oxide), were used to displace the weakly bound axial water ligands to form the one-dimensional polymers. The three one-dimensional polymers have been characterized by X-ray crystallography, and their basic structure was found to resemble that of the parent, *cis*-$Re_2(O_2CCH_3)_2Cl_4(H_2O)_2$.[61] The Re−Re distances occur in the range 2.236−2.251 Å and are characteristic of a Re−Re quadruple bond. Although the pyrazine- and 4,4′-bipyridine-linked polymers are not conducting in the neutral form, both exhibit electrical conductivity after oxidative doping with bromine vapor.

A one-dimensional polymer containing quadruply bonded dirhenium units linked by formate groups was prepared by adding triethylamine dropwise to a solution of $(NH_4)_2Re_2Cl_6$·$(HCOO)_2$.[88]

Dunbar, Walton, and co-workers again took advantage of the lability of the H_2O ligands in *cis*-$Re_2(O_2CCH_3)_2Cl_4(H_2O)_2$ to prepare two examples of chains of dirhenium units held together by hydrogen bonds. The axial water ligands are readily displaced by isonicotinamide ligands (INA) to form *cis*-$Re_2(O_2CCH_3)_2Cl_4(INA)_2$.[89] The Re−Re distance of 2.2493(4) Å is characteristic of a Re−Re quadruple bond and is slightly longer than the Re−Re bond in the $Re_2(O_2CCH_3)_2Cl_4(H_2O)_2$ starting material. The adjacent amide−amide hydrogen bonds serve to stitch the individual *cis*-$Re_2(O_2CH_3)_2Cl_4(INA)_2$ molecules into an infinite chain. The self-complementary bonding ability of the amide group situated in the 4 position of the pyridine ring of the isonicotinamide ligand results in the formation of a 1-D polymeric network. A similar reaction between $Re_2(O_2CCH_3)_2Cl_4(H_2O)_2$ and nicotinamide (NIA) produces the compound *cis*-$Re_2(O_2CCH_3)_2Cl_4(NIA)_2$·2NIA.[89] This compound crystallizes with two molecules of nicotinamide in the interstices. The amide groups in the 3 position on the pyridine ring are engaged in head-to-head hydrogen bonding. The *syn* disposition of the NIA ligands on each dirhenium unit leads to hydrogen bonds that form a sinusoidal pattern.

3. M_2 Starting Materials with a Bond Order of 3.5

3.1. Dimers of "Dimers"

The Re_2^{6+} synthon *cis*-$Re_2(\mu\text{-}O_2CCH_3)_2Cl_4(H_2O)_2$ reacts with bis[2-(diphenylphosphino)phenyl]ether (L_1)[90,91] and 2,6-bis(diphenylphosphinomethyl)-pyridine (L_2)[91] in refluxing ethanol to give paramagnetic complexes of the form $Re_2(\mu\text{-}O_2CCH_3)Cl_4(\eta^3\text{-}L_n)$ ($n = 1$ or 2) with a Re−Re bond order of 3.5.[90] The reducing agent for the process is probably the ethanol solvent. These compounds have been shown to react with terephthalic acid to yield $[Re_2Cl_4(\eta^3\text{-}L_1)]_2(\mu\text{-}O_2CC_6H_4CO_2)$ and $[Re_2Cl_4(\eta^3\text{-}L_2)]_2(\mu\text{-}O_2CC_6H_4CO_2)$, respectively. The dimers of "dimers" retain the same type of $Re_2(\mu\text{-}O_2CCH_3)_2Cl_4(\eta^3\text{-}L_n)$ structure that is present in the dinuclear starting material. The molecule $[Re_2Cl_4(\eta^3\text{-}L_1)]_2(\mu\text{-}O_2CC_6H_4CO_2)$ possesses an inversion center on the phenyl ring of the bridging terephthalate and has a Re−Re distance of 2.2424(4) Å, which is similar to the distances encountered in the dinuclear $Re_2(\mu\text{-}O_2CCH_3)Cl_4(\eta^3\text{-}L_n)$ compounds. In the structure of $[Re_2Cl_4(\eta^3\text{-}L_1)]_2(\mu\text{-}O_2CC_6H_4CO_2)$, the deviation of planarity of the $[Re_2O_2CC_6H_4CO_2Re_2]$ unit is reflected in the O−C−C−C and C−C−C−O torsion angles of 11.4° and 13.3°, respectively.[90] The redox potentials of the dimers of "dimers" are similar to those of the dinuclear starting materials; however, each of the processes show clear evidence of broadening due to the electronic coupling between the pairs of $[Re_2]^{5+}$ units. The pairs of one-electron redox processes could not be resolved, and the $\Delta E_{1/2}$ was estimated to be less than 40 mV for both $E_{1/2}$(ox) and $E_{1/2}$(red). Accordingly, the value of K_c is significantly less than 100, which is the same order of magnitude as expected for a weakly coupled valence-trapped system.

The dirhenium(II,III) complex, $Re_2(\mu\text{-}O_2CCH_3)Cl_4(\mu\text{-dppm})_2$, which contains the substitutionally labile acetate ligand in combination with the substitutionally inert dppm and Cl ligands, reacts with the dicarboxylic acids terephthalic acid, adipic acid, 4,4′-biphenyldicarboxylic acid, and fumaric acid to produce dimers of "dimers" of the form $[Re_2Cl_4(\mu\text{-dppm})_2]_2(\mu\text{-dicarboxylate})$.[92,93] The $\Delta E_{1/2}$ of 100 mV for the terephthalate bridge corresponds to a $K_c = 49$, which is characteristic of a weakly coupled valence-trapped system. The 4,4′-biphenyldicarboxylate-bridged analogue has a $\Delta E_{1/2}$ of 40 mV, a value that implies the absence of any significant coupling between the dirhenium units. The fumarate-linked dimer of "dimers" has a $\Delta E_{1/2}$ of 130 mV, which corresponds to a K_c value of 158, indicating the presence of stronger coupling relative to the case of the terephthalate-bridged species. The determination of a K_c value for the adipate-bridged compound was precluded by its poor solubility.[93]

The analogous reaction of $Re_2(\mu\text{-}O_2CCH_3)Cl_4(\mu\text{-dppm})_2$ with acetylenedicarboxylic acid gave the paramagnetic μ-η^2-acetylene complex, $Re_2Cl_5(\mu\text{-HCCH})(\mu\text{-dppm})_2$, resulting from the decarboxylation of

the acetylenedicarboxylic acid. The reaction of $Re_2(O_2CCH_3)Cl_4(dppm)_2$ with an excess of 1,4-cyclohexanedicarboxylic acid unexpectedly gave the dirhenium(II,II) complex, $Re_2(\mu\text{-}O_2CC_6H_{10}CO_2Et)_2Cl_2(\mu\text{-}dppm)_2$, rather than the expected dimer of "dimers". Attempts to prepare other examples of dimers of "dimers" by reacting $Re_2(O_2CCH_3)Cl_4(dppm)_2$ with perfluoroterephthalic acid and 1,1′-ferrocenedicarboxylic acid afforded $Re_2Cl_4(\mu\text{-}dppm)_2$.[93]

4. M_2 Starting Materials with a Bond Order of 3

4.1. Tetranuclear Clusters of Molybdenum and Tungsten

The coupling or oligomerization of M−M triple bonds has been a topic of long-standing interest to the Chisholm group, and indeed, in 1978, they speculated about the reversibility of a reaction wherein a metathesis of M≡M bonds could occur as in eq 15.

$$Cp_2Mo_2(CO)_4 + Cp_2W_2(CO)_4 = 2[Cp_2MoW(CO)_4] \quad (15)$$

However, studies of the species present in solution upon both thermal and photochemical excitation provided no evidence for the metathesis product, $Cp_2MoW(CO)_4$, despite the fact that it is formed in a thermal or photochemical reaction employing $Cp_2M_2(CO)_6$ compounds (M = Mo and W).[5] After this early work, several M_4 clusters were formed by the coupling of two M≡M units when supported by alkoxide ligands.

The reversible coupling of two $W_2(O^iPr)_6$ molecules was discovered in 1986,[94] while the addition of secondary and bulky primary alcohols (^{i}Pr, $CH_2{}^t$Bu, $CH_2{}^cC_5H_9$, $CH_2{}^cC_4H_7$, and $CH_2{}^i$Pr) to $W_2(O^tBu)_6$ was shown to yield black crystalline clusters $W_4(OR)_{12}$ and/or $W_4(OR)_{12}(HOR)$.[95] The molybdenum analogues $Mo_4(OR)_{12}$ and $Mo_4(OR)_{12}(HOR)$ are also formed for the less sterically demanding alkyl ligands but not for R = ^{i}Pr and $CH_2{}^t$Bu, which remain as dinuclear species.[96−97]

The compound $W_4(O^iPr)_{12}$ was crystallographically characterized along with $W_2(O^iPr)_6$: the unit cell contained one dinuclear and one tetranuclear species.[94] The tetranuclear structure is shown in Figure 22. The central W_4 unit is diamond-shaped, having alternating short, 2.5 Å, and long, 2.8 Å, W−W distances, with a significant backbone W−W interaction, 2.7 Å. The low temperature ^{1}H NMR spectrum is consistent with expectations based on the C_{2h} symmetry found in the solid state. Upon raising the temperature, two dynamic processes are observed, one of which is intramolecular and the other of which involves the reversible dissociation of the tetranuclear compound to $W_2(O^iPr)_6$ (eq 16).

$$W_4(O^iPr)_{12} \rightleftarrows 2[W_2(O^iPr)_6] \quad (16)$$

The intramolecular process involves the site exchange of the bridging alkoxides without exchange with the terminal O^{i}Pr ligands. Also, one set of terminal groups exchange sites, but these do not exchange with the other set of terminal groups. An

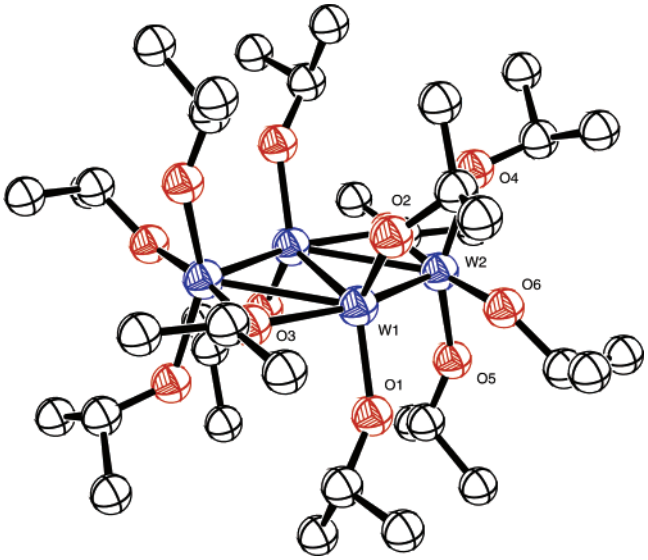

Figure 22. Molecular structure of the $W_2(O^iPr)_6$ dimer. Hydrogen atoms omitted for clarity. Only one set of symmetry-equivalent atoms is labeled.

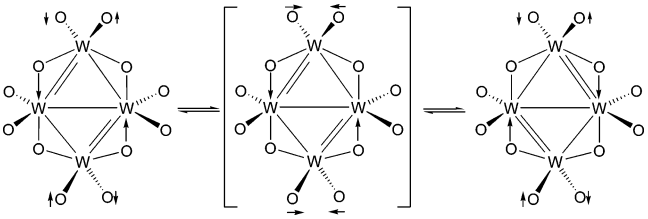

Figure 23. The"Bloomington Shuffle"

inspection of the terminal groups allows one to see that the O^{i}Pr ligands of the wing-tip W atoms may be classified in a pairwise manner as proximal and distal with respect to the orientation of the methine vector. The terminal O^{i}Pr ligands of the wing-tip W atoms thus interconvert, as do the bridging groups, but these transformations do not involve the O^{i}Pr groups of the backbone W atoms. The explanation proposed for this dynamic process was that the C_{2h} W_4 cluster oscillates about the more symmetric diamond W_4 structure wherein the W−W distances are equivalent. This leads to the bridging groups becoming equivalent without exchange with the terminal groups. Concomitant with this dynamic process is a correlated motion of the wing-tip O^{i}Pr groups. The process is shown schematically in Figure 23 and was called the Bloomington Shuffle.[98] The energy of activation of this intramolecular process could reasonably be estimated to be ca. 13 kcal mol^{-1} from the line-broadening seen at low temperatures. However, at room temperature, the equilibrium shown in eq 16 is clearly evident by NMR spectroscopy (although it is never rapid on the NMR time scale).

From detailed studies of the reaction in eq 16, the thermodynamic parameters $\Delta H° = -16$ kcal mol^{-1} and $\Delta S° = +60$ eu were obtained, together with the activation parameters $\Delta H^{\neq} = 5$ kcal mol^{-1} and $\Delta S^{\neq} = +38$ eu for the forward (dissociative) reaction and $\Delta H^{\neq} = 10$ kcal mol^{-1} and $\Delta S^{\neq} = -40$ eu for the back-(associative) reaction. Clearly, the cluster is favored on enthalpic grounds but disfavored by entropy. The

low enthalpic barrier to the association of two M≡M bonds is noteworthy and contrasts with the case of simple $p_\pi - p_\pi$ systems for which the process would be symmetry forbidden by the Woodward−Hoffmann rules.

The analogy with cyclobutadiene for the W_4-12 electron clusters was also made in a theoretical analysis of the bonding in the cluster.[98] The descent from D_{4h} to C_{2h} symmetry was reasonably traced to a second-order Jahn−Teller distortion. The preference for the diamond W_4 geometry relative to the rectangular C_4H_4 ground-state structure could also be traced to the importance of Wd−Wd orbital interactions which favor the diamond where W−W backbone M−M bonding can contribute to cluster stabilization.

The $W_4(O^iPr)_{12}$ cluster appears to be unique among the $M_4(OR)_{12}$ clusters in two respects. (1) It is the only one so far to exhibit an equilibrium of the type shown in eq 16. (2) The NMR spectra of other compounds of formula $M_4(OR)_{12}$ (M = Mo, W) cannot be rationalized by a similar structure but rather by the adoption of the M_4-butterfly structure depicted in **V**, where O represents an alkoxide ligand.

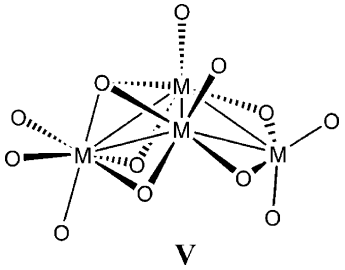

V

Structure **V** has a marked asymmetric distribution of RO ligands, implying that the oxidation states of the metal atoms are not all the same. This asymmetry is also reflected in the Mo−Mo distances seen in the structure of the alcohol adduct $Mo_4(OCH_2{}^c\text{-}Bu)_{12}(HOCH_2{}^c Bu)$ shown in Figure 24.[97] Structure **V** is thus seen to be related to that shown in Figure 24 by the loss of the HOR ligand.

The reaction between $Mo_2(O^iPr)_6$ and acetyl chloride or Me_3SiCl in hexane leads to a black insoluble compound that was characterized by single X-ray crystallography as $Mo_4Cl_4(O^iPr)_8$.[99] The molecule has a crystallographically imposed C_4 axis. There are four terminal Mo−Cl bonds and eight bridging O^iPr ligands, four lying above and four lying below a Mo_4 square. Quite remarkably, the related compound $Mo_4Br_4(O^iPr)_8$, prepared in a similar manner but with Me_3SiBr, has a butterfly-Mo_4 unit with terminal Mo−Br bonds and edge- and face-bridging alkoxides.[99] The chloride and bromide structures are shown in Figures 25 and 26, respectively. The structures of $Mo_4X_3(O^iPr)_9$ molecules, X = Cl, Br, and I, also prepared in reactions involving Me_3SiX, can be reliably traced to the butterfly structure (by NMR spectroscopy), and this was established by crystallography for X = Br, wherein one of the wing-tip terminal Mo−Br bonds is replaced by a terminal O^iPr group.[100]

The bonding in these molecules was examined by Fenske−Hall MO calculations wherein OH was substituted for O^iPr. The square and butterfly structures

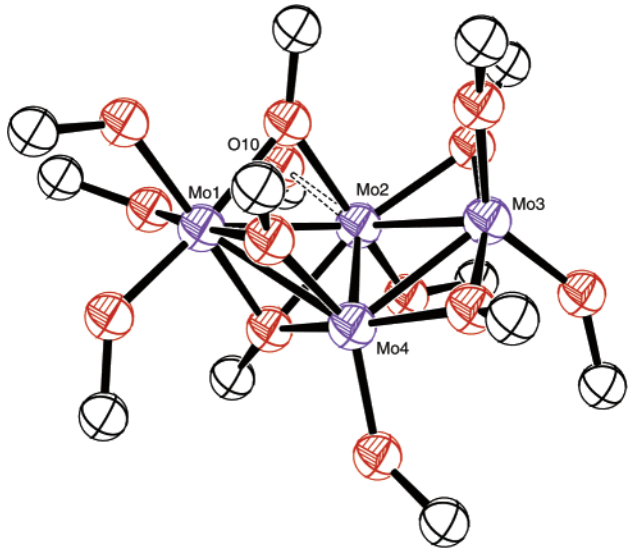

Figure 24. Molecular structure of $Mo_4(OCH_2{-}c\text{-}Bu)_{12}(HOCH_2{-}c\text{-}Bu)$. The cyclobutyl rings and methylene hydrogen atoms have been omitted for clarity. The molybdenum atoms, along with the alcohol oxygen atom (O10), are labeled.

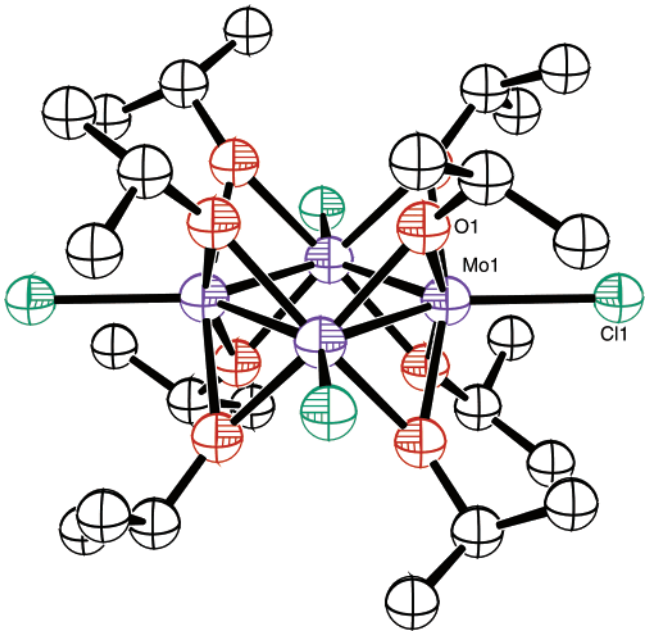

Figure 25. Molecular structure of $Mo_4Cl_4(O^iPr)_{12}$. Hydrogen atoms have been omitted for clarity, and only one set of symmetry-equivalent Mo, O, and Cl atoms is labeled.

are related by being fragments of the well-known cube-octahedral clusters $M_6(\mu_3\text{-}X)_8L_6$.[101] The preference for Mo−halide bonds to occupy terminal sites can be understood in terms of maximizing M−M bonding within the cluster. The ligands with weaker *trans* influence, in this case Cl or Br, relative to O^iPr, occupy positions wherein they do not compete as effectively for metal d orbitals, which can otherwise be used in M−M bonding.

The unusual cluster $W_4(p\text{-tolyl})_2(O^iPr)_{10}$ was obtained by adding ^{i}PrOH to hexane solutions of $W_2(p\text{-tolyl})_2(NMe_2)_4$.[102] This cluster has a planar central W_4 moiety with an "open edge" in the sense that two tungsten atoms are held together through the agency

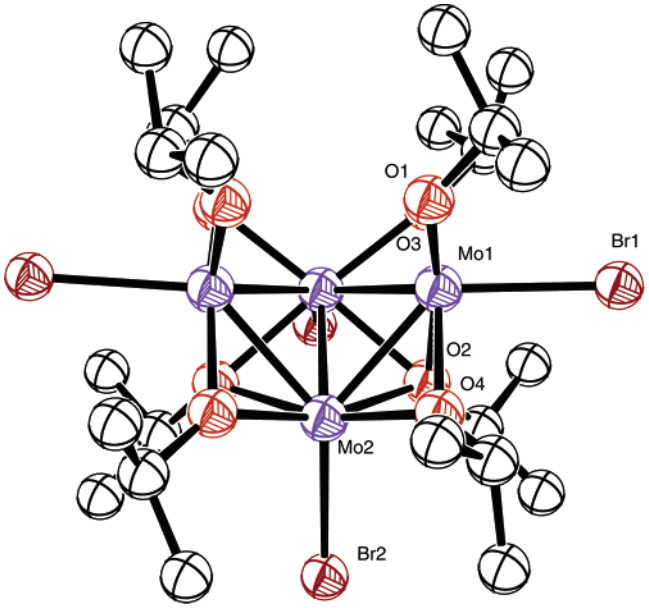

Figure 26. Molecular structure of $Mo_4Br_4(O^iPr)_{12}$. Hydrogen atoms have been omitted for clarity, and only one set of symmetry-equivalent Mo, O, and Br atoms has been labeled.

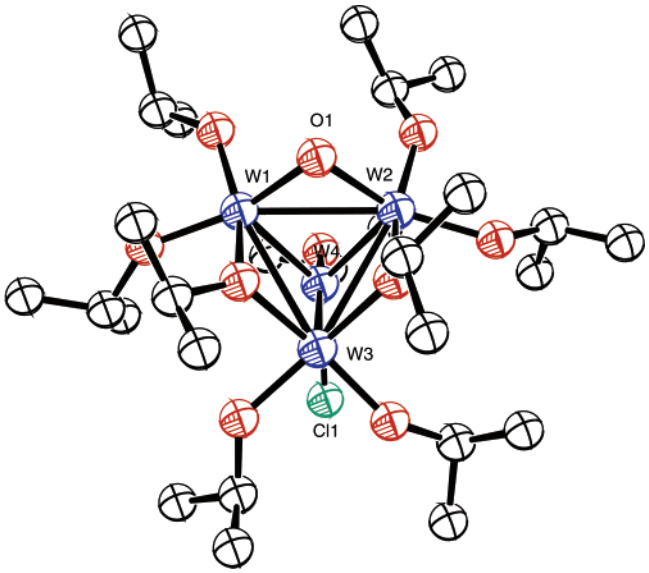

Figure 27. Molecular structure of $W_4(\mu_2\text{-}O)(Cl)(O^iPr)_9(Et_2O)$. The hydrogen atoms and Et_2O solvent molecule are omitted for clarity. The W, Cl, and bridging O atoms are labeled.

of an alkoxide bridge rather than by a direct M−M bond. The structure may be viewed as a rather strange perturbation of the $W_4(O^iPr)_{12}$ structure described previously.

Two other 12-electron W_4 clusters, $W_4O(X)(O^iPr)_9$, where X = Cl or O^iPr were obtained from degradation of $W_4(O^iPr)_{12}$ upon heating in solution.[103,104] By ^1H NMR spectroscopy, they were found to be structurally related, although only the cluster $W_4(O)X(O^iPr)_9$ where X = Cl was characterized by an X-ray study.[103] The structure is shown in Figure 27. A $WCl(O^iPr)$ unit caps a triangular $W_3(\mu\text{-}O)(\mu\text{-}O^iPr)_2(O^iPr)_6$ moiety. The W−W distances in the latter are all long, while the three W−W distances to the capping tungsten

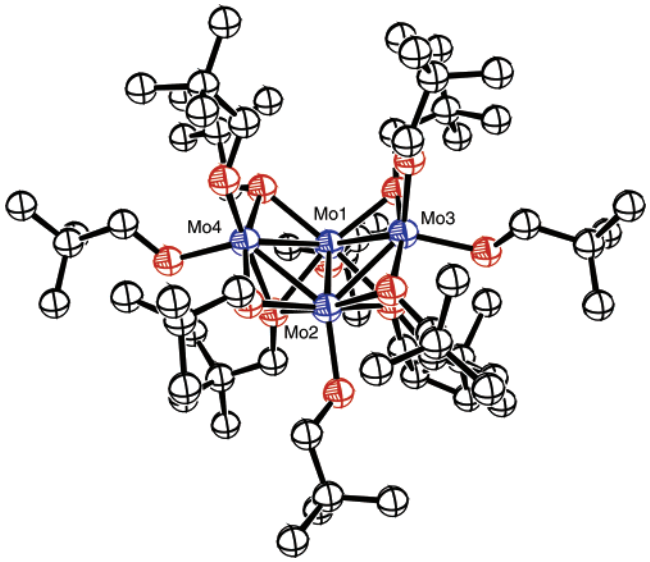

Figure 28. Molecular structure of the $[Mo_4(\mu_4\text{-}H)(OCH_2{}^tBu)_{12}]^{1-}$ butterfly anion as found in the molecular structure of $[K(crown)\cdot 2THF][Mo_4(\mu_4\text{-}H)(OCH_2{}^tBu)_{12}]$. The hydride atom was not located crystallographically but is known to bridge the four Mo atoms. The hydrogen atoms and the entire cation are omitted for clarity. The Mo_4 framework is labeled.

atom are short, indicative of some multiple bond order.

The addition of the hydride anion from either KH or $NaHBEt_3$ in THF/18-crown-6 to solutions of $Mo_2(OR)_6$, where R = ^{i}Pr[105] and $CH_2{}^tBu$,[106] leads to the formation of the cluster anion $Mo_4(\mu_4\text{-}H)(OR)_{12}$, whose structure is shown in Figure 28. Evidently, addition of H^- to $Mo_2(OR)_6$ yields a nucleophilic $[Mo_2(H)(OR)_6]^-$ moiety which associates with another $Mo_2(OR)_6$ molecule. The structure is related to that seen for $Mo_4Br_4(O^iPr)_8$. Evidence for the μ_4-H ligand comes from both crystallographic data and MO calculations.[105,106]

Two other clusters derived from $(M{\equiv}M)^{6+}$ centers warrant mention. The hydrogenation of $W_2(^i Bu)_2(O^iPr)_4$ in hydrocarbon solvents leads to a most unusual cluster hydride: $W_6(H)_5(C^iPr)(O^iPr)_{12}$.[107] This compound was originally formulated[108] as $W_6(H)_5(O^iPr)_{13}$, but a more carefully crystallographic refinement and a detailed ^{13}C [^1H] study revealed the presence of the μ-C^iPr ligand. The compound is unusual in having five hydride ligands, four of which are edge bridging a W_6 octahedron with one terminal. Each edge of the octahedron has a bridging group (H, O^iPr, or C^iPr), and each terminal site, an O^iPr or H ligand. The compound is not fluxional and is, in fact, relatively inert, so that site-selective hydrogenolysis and ethylene hydrogenation was observed for the terminal W−H group. The other cluster is $Mo_4(H)_3(O^tBu)_7(HNMe_2)$ formed in a hydrogenation of a $Mo_2(p\text{-tolyl})_2(NMe_2)_2(O^tBu)_2/Mo_2(p\text{-tolyl})_2(NMe_2)_4$ mixture in hexane/^{t}BuOH at room temperature.[109,110] This molecule has a Mo_4-butterfly arrangement of metal atoms. One triangular face has a two edge-bridging (μ_3)-hydride ligands and one face-capping (μ_3)-hydride ligand in addition to terminal OR (backbone) and $HNMe_2$ (wing-tip) ligands, while the other triangle has only edge-bridging and terminal OR

groups. In this reaction, the conversion of an amide ligand to an amine and liberation of toluene leads to a 14-electron cluster count as the average oxidation number for molybdenum goes from 3 to 2.5.

Interesting analogies in the bonding of early transition metal alkoxide clusters and later transition metal carbonyl clusters have been noted. However, perhaps the most amazing thing about these 12-electron clusters of molybdenum and tungsten formed formally from the coupling of two M≡M units is the variety of geometries seen for the M_4 unit. Clearly, the M—M bonding is very sensitive or responsive to the steric and electronic constraints of the attendant ligands. This is even further underscored by a consideration of the linked M≡M bonded dimers described below, where localized multiple bonds persist and are preferred because of electronic or steric factors.

4.2. Dimers of M–M Triple Bonds

It was previously noted that $Mo_2(O^iPr)_6$ does not show any tendency to form $Mo_4(O^iPr)_{12}$, akin to its tungsten analogue (eq 16). However, with less sterically demanding alkoxide ligands, clusters are formed as shown for $Mo_4(OCH_2{}^cBu)_{12}(HOCH_2{}^cBu)$ in Figure 24. In an attempt to study the nature of the "dimerization" process, $Mo_2(O^iPr)_6$ and MeOH were allowed to react in hydrocarbon solvents. An initial dimer of "dimers" was characterized, $[Mo_2(O^iPr)_4(\mu\text{-OMe})(\mu\text{-}O^iPr)]_2$.[111] See Figure 29. Here the rectangular Mo_4

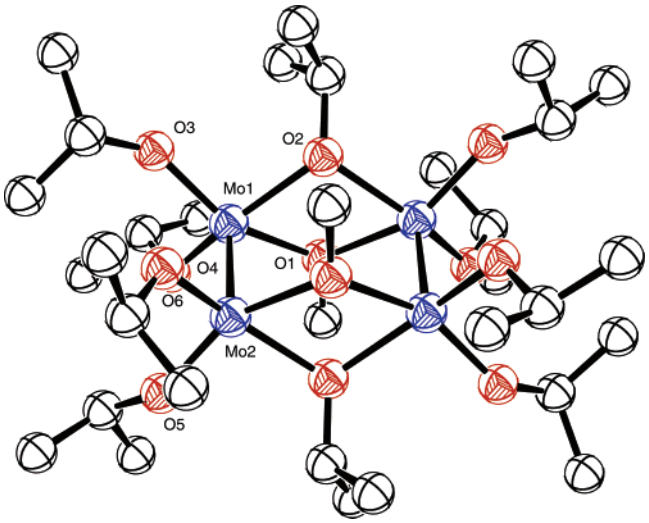

Figure 29. Molecular structure of the mixed alkoxide cluster $Mo_4(\mu_2\text{-OMe})_2(\mu_2\text{-}O^iPr)_2(O^iPr)_8$. Hydrogen atoms are omitted for clarity. Only one set of symmetry-equivalent atoms is labeled.

unit contains two localized Mo≡Mo bonds of distance 2.22 Å brought together by alkoxide bridges with nonbonding Mo···Mo distances of 3.5 Å.

A similar rectangular Mo_4-containing molecule was obtained from the reaction between $Mo_2(O^iPr)_6$ and PF_3 (2 equiv) in a hydrocarbon solvent, namely $[Mo_2(O^iPr)_4(\mu\text{-}O^iPr)(\mu\text{-F})]_2$.[100] Here the dimer of "dimers" was readily cleaved by the addition of PMe_3, which gave $Mo_2(O^iPr)_6$ and $Mo_2F_2(O^iPr)_4(PMe_3)_2$. Treatment of a hydrocarbon solution of $Mo_2(O^tBu)_6$ with PF_3 (2 equiv) gave $Mo_4(\mu\text{-F})_4(O^tBu)_8$, whose

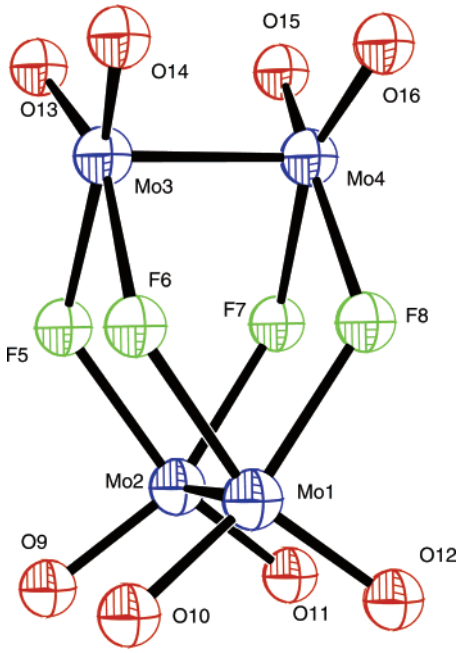

Figure 30. Molecular structure of $Mo_4F_4(O^tBu)_8$. ^{t}Bu methyl groups are omitted for clarity, and the Mo, O, and F framework is labeled.

structure is depicted in Figure 30.[112] Once again, the Mo—Mo distances of 2.25 Å and 3.7 Å leave no doubt that the localized triple bonds have been retained. This is further supported by the fact that treatment of $Mo_4(\mu\text{-F})_4(O^tBu)_8$ with PMe_3 (4 equiv) yields $Mo_2(F)_2(O^tBu)_4(PMe_3)_2$.[113] These reactions are shown in eqs 17 and 18. A minor impurity was also identified as a related cluster, $Mo_4(\mu\text{-F})_3(\mu\text{-}NMe_2)(O^tBu)$.[100]

$$2[Mo_2(O^tBu)_6] + 4PF_3 \rightarrow Mo_4F_4(O^tBu)_8 + 4PF_2O^tBu \quad (17)$$

$$Mo_4F_4(O^tBu)_8 + 4PMe_3 \rightarrow 2[Mo_2(F)_2(O^tBu)_4(PMe_3)_2] \quad (18)$$

A somewhat similar bis-phenoid of Mo_4 atoms is seen in the structure of $Mo_4(\mu\text{-O})_2(CH_2SiMe_3)_8$. See Figure 31. This oxo-linked dimer of "dimers" is formed in the reaction shown in eq 19.[114]

$$2Mo_2Br_2(CH_2SiMe_3)_4 + 2H_2O + 4{}^iPr_2NH \rightarrow Mo_4(\mu\text{-O})_2(CH_2SiMe_3)_8 + 4{}^iPr_2NHBr \quad (19)$$

The notable feature of the structure in Figure 31 is that each molybdenum atom is three-coordinate and the local ethane-like $Mo_2O_2C_4$ core is *gauche*, whereas, in the previously described linked Mo_2^{6+} species, the coordination about each Mo atom is four, such that each $L_4Mo{\equiv}Mo$ unit is square pyramidal.[114]

The addition of alcohols to $W_2(COT)(NMe_2)_4$ leads to $[W_2(COT)(OR)_4]_2$ compounds, where R = Me, Et, and *n*-Pr and COT = 1,3,5,7-cyclooctatetraene. The molecular structure of the *n*-propoxide is shown in Figure 32.[115] The WW triple bond of distance 2.3917(2) Å is rather long, although the presence of both bridging OR and COT ligands perturbs the simple

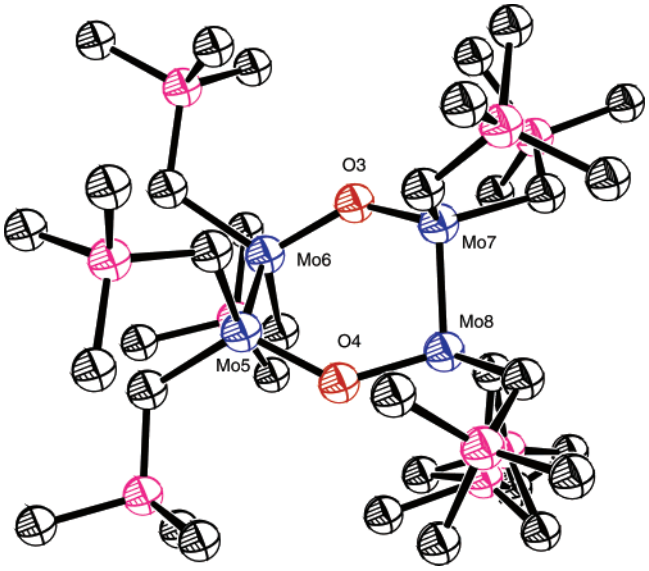

Figure 31. Molecular structure of one of the independent molecules of $Mo_4(\mu_2\text{-}O)_2(CH_2SiMe_3)_8$. The hydrogen atoms are omitted for clarity, and the molybdenum and oxygen core is labeled.

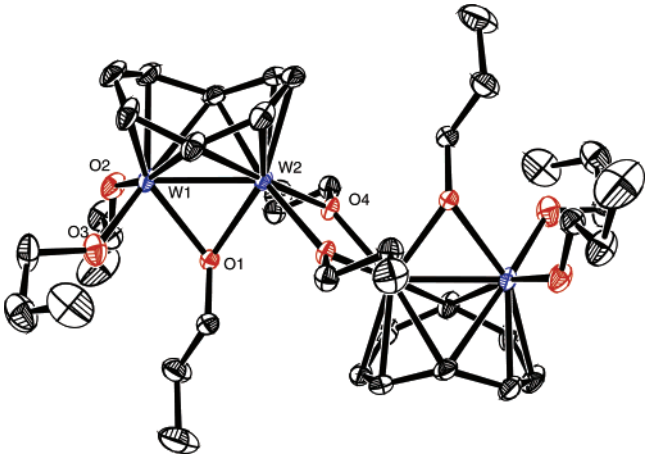

Figure 32. Molecular structure of $[W_2(\mu\text{-}\eta^5,\eta^5\text{-COT})(OPr)_4]_2$. Only one set of symmetry-equivalent atoms is labeled. Hydrogen atoms are omitted for clarity, and thermal ellipsoids are drawn at the 30% probability level.

description of a MM triple bond, having one σ component and two equivalent π components. The central W···W distance of 3.3986(2) Å, which is bridged by a pair of OR ligands, is clearly a nonbonding distance.

The electron-rich MM triply bonded complex, $Re_2Cl_4(dppm)_2$, of MM configuration $\sigma^2\pi^4\delta^2\delta^{*2}$, reacts with TCNQ in THF or CH_2Cl_2 to give a black crystalline charge-transfer complex, $[Re_2Cl_4(dppm)_2]_2(\mu\text{-TCNQ})$, where the bridging TCNQ ligand occupies equatorial sites, and one Re atom of each dinuclear center has an axial Re−Cl bond, as shown in Figure 33.[116] The compound was noted to be paramagnetic on the basis of both magnetic susceptibility measurements and EPR spectroscopy, and it was formulated as a charge-transfer complex with a partially reduced TCNQ ligand.

A 1,4-cyclohexanedicarboxylate-bridged dimer of "dimers", $[Re_2Cl_2(\mu\text{-dppm})_2(\mu\text{-}O_2C_6H_{10}CO_2H)]_2(\mu\text{-}O_2CC_6H_{10}CO_2)$, can be prepared by reacting *cis*-$Re_2(\mu\text{-}O_2CCH_3)_2Cl_2(\mu\text{-dppm})_2$ with an excess of *trans*-1,4-cyclohexanedicarboxylic acid.[92] The crystal structure of the complex reveals an interesting polymeric structure in which dimer of "dimers" units are held together through intermolecular hydrogen bonds involving the "free" carboxylic acid groups to generate zigzag chains. The $[Bu_4N]^+$ salt of the complex was shown to react with $[Re_2Cl_4(\mu\text{-dppm})_2(NCCH_3)_2]BF_4$ to yield the paramagnetic octanuclear chain complex $[(\mu\text{-dppm})_2Cl_4Re_2(\mu\text{-}O_2CC_6H_{10}CO_2)Re_2Cl_2(\mu\text{-dppm})_2]_2(\mu\text{-}O_2CC_6H_{10}CO_2)$.[92]

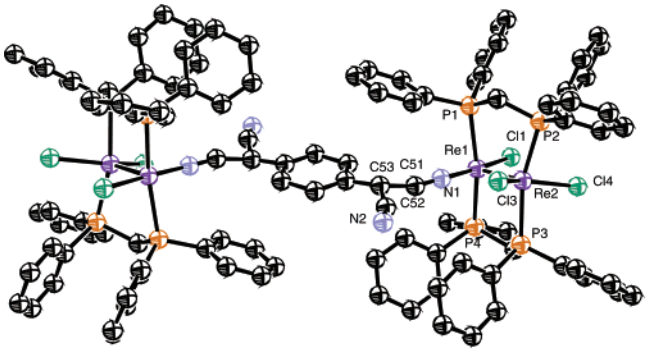

Figure 33. Molecular structure of $[Re_2Cl_4(dppm)_2]_2(\mu\text{-TCNQ})$. Hydrogen atoms are removed for clarity, and one set of symmetry-equivalent core atoms is labeled.

Attempts to prepare the $Os_2I_8^{2-}$ anion by reacting $[PMePh_3]_2Os_2Cl_8$ with HI in an analogous fashion to the conversion of $Re_2Cl_8^{2-}$ to $Re_2I_8^{2-}$ resulted instead in the formation of the $Os_2I_{14}^{2-}$ anion. The molecular structure of the anion is shown in Figure 34. There are two staggered Os_2I_8 units, Os−Os = 2.23(1) Å, fused together along a common edge.[117]

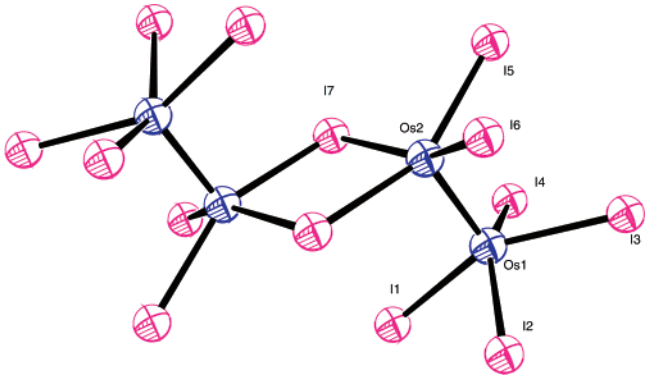

Figure 34. Molecular structure of the $Os_2I_4^{-1}$ anion as found in $[Ph_3PMe][Os_2I_{14}]$. The cation is omitted, and one set of symmetry-equivalent atoms is labeled.

4.3. Triangles and Squares

"Hybrid" molecular squares containing Re_2^{4+} units were prepared by reacting *cis*-$Re_2Cl_2(\mu\text{-dppm})_2(\mu\text{-}O_2CC_5H_4N)_2$ in a 1:1 ratio with *cis*-$Pt[P(C_2H_5)_3]_2(O_3SCF_3)_2$, $Pt(dbbpy)(O_3SCF_3)_2$ (dbbpy = 4,4′-di-*tert*-butyl-2,2′-bipyridine), and $ZnCl_2$ to yield [*cis*-$Re_2Cl_2(\mu\text{-dppm})_2(\mu\text{-}O_2CC_5H_4N)_2\{Pt[P(C_2H_5)_3]_2\}_2[O_3SCF_3]_4$,[118] [*cis*-$Re_2(O_3SCF_3)_2(\mu\text{-dppm})_2(\mu\text{-}O_2CC_5H_4N\text{-}4)]_2\{Pt(dbbpy)\}_2(O_3SCF_3)_4$,[118] and [{*cis*-$[Re_2Cl_2(dppm)_2(O_2CC_5H_4N\text{-}4)_2]\}\{ZnCl_2\}]_2$,[119] respectively. The latter two compounds have been structurally characterized.[118,119] The structure of the cationic unit of [*cis*-$Re_2(O_3SCF_3)_2(\mu\text{−dppm})_2(\mu\text{-}O_2CC_5H_4N)Pt(dbbpy)]_2[O_3$-

$SCF_3]_4$ is a molecular square consisting of alternating $[(dppm)_2Re^{II}_2]$ and $[(dbbpy)Pt^{II}]$ units at the verticies and isonicotinate ligands along the edges. The molecule is considerably distorted from ideality; the Pt−Pt diagonal is 11.97 Å, whereas the diagonal defined by the midpoints of the two Re_2 units is 13.26 Å. The vertex angles subtended by the Re_2 units are less than 90°, a situation that leads to a bending of the isonicotinate ligands to accommodate ring closure. The $[cis\text{-}Re_2Cl_2(dppm)_2(O_2CC_5H_4N\text{-}4)_2]\{ZnCl_2\}$ complex is a molecular square consisting of alternating $(dppm)_2ReCl_2$ and $ZnCl_2$ units at the verticies and isonicotinate ligands along the edges. As with the Pt-containing species, the square is considerably distorted, as evidenced by the Zn···Zn diagonal distance of 11.881(5) Å, and the diagonal defined by the midpoints of the two Re_2 units is 13.608(3) Å. These distances are strikingly similar to those of the Pt-containing analogue. The Re−Re, Re−P, Re−O, and Re−Cl distances in the Zn-containing square are similar to the corresponding distances in the precursor complex, $cis\text{-}[Re_2Cl_2(dppm)_2(O_2CC_5H_4N\text{-}4)_2]$.

Cyclic voltammetric studies revealed that both Pt-containing squares exhibited two reversible one-electron oxidations. The $\Delta E_{1/2}$ value of 130 mV for both complexes corresponds to a K_c value of 158, which is indicative of weak electronic coupling of the Re_2^{4+} units through the Pt^{II} centers.[118]

The reaction of $cis\text{-}Re_2(\mu\text{-}O_2CCH_3)_2Cl_2(\mu\text{-}dppm)_2$ with terephthalic acid afforded $\{[Re_2Cl_2(\mu\text{-}dppm)_2](\mu\text{-}O_2CC_6H_4CO_2)\}_3$, which contains a triangle of Re_2^{4+} units. The complex has been structurally characterized.[92] The three Re−Re bond distances are essentially identical (2.319 Å) and are similar to the distance 2.2763(7) Å in the parent complex. The CV of the complex exhibits two sequential oxidations with $E_{1/2}$ values (vs Ag/AgCl) of ~400 mV and +330 mV.[92] These are associated with the net three-electron oxidation that is possible for the $[Re_2^{4+}]_3$ core.

4.4. Polymers

In contrast to the reactions described in section 4.3, $cis\text{-}[Re_2Cl_4(dppm)_2(O_2CC_5H_4N\text{-}4)_2]$ reacts with $Ag(O_3SCF_3)$, $cis\text{-}[Re_2Cl_4(O_2CCH_3)_2(H_2O)_2]$, and $[Rh_2(O_2CCH_3)_4]$ to yield open-chain polymeric structures, $[\{cis\text{-}Re_2(OReO_3)_2(dppm)_2(O_2CC_5H_4N\text{-}4)_2\}\{Ag\cdot ReO_4\}]_\infty$, $[\{cis\text{-}Re_2Cl_2(dppm)_2(O_2CC_5H_4N\text{-}4)_2\}\{cis\text{-}Re_2Cl_4(O_2CCH_3)_2\}]_\infty$, and $[\{cis\text{-}Re_2Cl_2(dppm)_2(O_2CC_5H_4N\text{-}4)_2\}\{Rh_2(O_2CCH_3)_4\}]_\infty$, respectively.[119] The reason why the reactions of $Ag(O_3CCF_3)$, $cis\text{-}[Re_2Cl_4(O_2CCH_3)_2(H_2O)_2]$, and $Rh_2(O_2CCH_3)_4$ with $cis\text{-}[Re_2Cl_2(dppm)_2(O_2CC_5H_4N\text{-}4)_2]$ yield polymers instead of squares may be related to the fact that squares of larger dimensions would require many solvent molecules to crystallize in the void space. Close-packed polymers also contain solvent molecules, but the packing of larger squares is expected to be much less efficient.[119]

5. M_2 Starting Materials with a Bond Order of 2.5

5.1. Dimers of "Dimers"

The Ru_2^{5+}-containing dimer of "dimers", $[\{Ru_2(chp)_4\}_2(\mu\text{-}pyz)][BF_4]_2$ (chp = anion of 6-chloro-2-hydroxypyridine), was prepared by substitution of the axial chloride ligand in $Ru_2(chp)_4Cl$ with pyrazine.[120] The Ru−Ru distance is 2.267(1) Å, and the RuN(pyz) distance is 2.275(5) Å. The Ru−Ru−N(pyz) linkage is essentially linear. The pyz molecule is strictly planar, and the pyz plane is only 8° away from being coplanar with the O−Ru−O−C−N−Ru−N−C plane. Magnetic susceptibility measurements show that there is no significant magnetic exchange interaction between the dinuclear species in the $[\{Ru_2(chp)_4\}_2(pyz)]^{2+}$ ion.

The reaction of $Ru_2(DAniF)_3(O_2CCH_3)Cl$, prepared by modifying the procedure used for $Mo_2(DAniF)_3(O_2CCH_3)$, or $Ru_2(DAniF)_4Cl$, with $(NBu_4)_2O_2CC_6H_4CO_2$ yields $[Ru_2(DAniF)_3Cl]_2(O_2CC_6H_4CO_2)$.[121] The two independent Ru−Ru bond distances of 2.3319(4) and 2.3258(5) Å are somewhat shorter than the Ru−Ru distances of the $Ru_2(formamidinate)_4Cl$ complexes but slightly longer than those in the mixed acetate/formamidinate complex, $cis\text{-}Ru_2(DAniF)_2(O_2CCH_3)_2Cl$, 2.319(1) Å. The dark blue $[Ru_2(DAniF)_3Cl]_2(O_2CC_6H_4CO_2)$ reacts with zinc powder in THF solution to produce a red reduced species, $[Ru_2(DAniF)_3Cl_{0.12}]_2(O_2C_6H_4CO_2)$.[121] The unique Ru−Ru distance of 2.4162(3) Å is significantly longer than the corresponding distance in the starting material and is clearly in the range of distances typical for Ru_2^{4+} complexes with bridging formamidinates.

The Ru_2^{5+} dimers of "dimers" linked by butadiynediyl and ethynediyl bridges have been prepared by treating $Ru_2(ap)_4Cl$ (ap = *N*,*N*′-2-anilinopyridinate) with LiCCCCLi and LiCCLi, respectively.[122] The complexes have been characterized by both elemental analysis and FAB mass spectrometry. In addition, the butadiynediyl-bridged compound has been structurally characterized. From the structure shown in Figure 35, a linear array formed by the bridging C_4

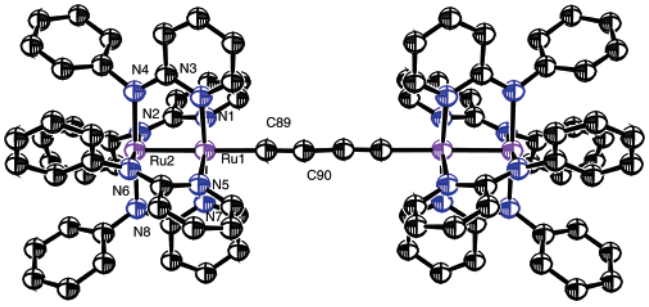

Figure 35. Molecular structure of one of the independent molecules of $[Ru_2(ap)_4]_2(\text{-}C{\equiv}C{-}C{\equiv}C\text{-})$. Hydrogen atoms are omitted for clarity, and one of the sets of symmetry-equivalent core atoms is labeled.

chain and the two terminal Ru_2^{5+} units is clearly evident. Some small but notable differences exist between the butadiynediyl-bridged complex and the dinuclear $Ru_2(ap)_4(C{\equiv}CSiMe_3)$: the Ru−Ru (2.331(2) Å) and $C_\alpha{\equiv}C_\beta$ distances are elongated in the butadiynediyl-bridged complex while the RuC_α distance is shortened relative to the case of the dinuclear species. Although barely significant, all of these changes are consistent with the strengthening of the $Ru{-}C_\pi$ interaction and concomitant weakening of the $\pi(C{\equiv}C)$ bond. Both the butadiynediyl- and ethynediyl-bridged complexes undergo four quasi-reversible one-

electron redox processes and one irreversible one-electron redox processes. Therefore, there are six accessible oxidation states for both complexes. The K_c values of 3.8×10^6 (red.) and 506 (ox.) for the butadiynediyl and 1.9×10^{11} (red.) and 6.6×10^4 (ox.) for the ethynediyl-bridged complexes indicate very strong coupling. The distance dependence of the coupling is evident in that K_c of the C_4-bridged complex is several orders of magnitude smaller than that for the C_2-bridged complex. Additionally, K_c(red.) is much larger than K_c(ox.) for the same complex, indicating that the Ru−C_π bonding is much stronger in the reduced form than in the oxidized form.

The reaction between $Ru_2(ap)_4Cl$ and a series of aryl acetylenes, 1,4-$C_6H_4(C{\equiv}CLi)_2$, 1,3-$C_6H_4(C{\equiv}CLi)_2$ and 1,3,5-$C_6H_3(C{\equiv}CLi)_3$, resulted in the formation of the Ru_2^{5+} dimers of "dimers" 1,4-$[Ru_2(ap)_4(C{\equiv}C)]_2C_6H_4$, 1,3-$[Ru_2(ap)_4(C{\equiv}C)]_2C_6H_4$, and 1,3-$[\{Ru_2(ap)_4(C{\equiv}C)\}_2]$-$C_6H_3$-5-C≡CH, respectively.[123] The complexes were characterized by FAB mass spectrometry, microanalysis, and UV−vis and IR spectroscopy. The complexes have magnetic moments of 5.51, 5.29, and 5.83 μ_B, respectively, which are consistent with a molecule containing two noninteracting $S = {}^3/_2$ centers. All three complexes exhibit three redox couples: an oxidation and two reductions. The oxidation and the first reduction are quasi-reversible. Instead of exhibiting pairwise redox waves similar to those recorded for $[Ru_2(ap)_4]_2(\mu\text{-}C_{2m})$ ($m = 1, 2$), the complexes display two-electron redox couples at potentials corresponding to those for the one-electron couples observed for the monoalkynyl adducts of $Ru_2(ap)_4$. This result may be interpreted as the absence of strong electronic coupling between the $Ru_2(ap)_4$ units bridged by aryl acetylides.

The dimer of "dimers" $[Ru_2(O_2CCH_3)_2(mhp)_2]_2(\mu$-DM-Dicyd) has been prepared by the reaction of 2 equiv of $[Ru_2(O_2CCH_3)_2(mhp)_2(MeOH)](BF_4)$ with 1 equiv of $[As(Ph)_4]_2$[DM-Dicyd] (DM-Dicyd = 1,4-dicyanamido-2,5-dimethylbenzene dianion).[124] The complex exhibits three redox waves: one quasi-reversible two-electron reduction, one reversible one-electron oxidation, and an irreversible one-electron oxidation. The first process is attributed to the simultaneous reduction of both Ru$_2$(II,III) units to Ru$_2$(II,II), indicating that there is no significant communication occurring through the bridging DM-Dicyd^{2-} ligand. The magnetic data for this compound revealed weak antiferromagnetic interaction ($g = 2.10$; $2J = -0.90$ cm^{-1}, $D = 75.0$ cm^{-1}).

The Os_2^{5+}-containing dimer of "dimers", $[\{Os_2(chp)_4\}_2(pyz)](BF_4)(CH_2Cl_2)(pyz)_2$, was prepared in a manner very similar to that used for the Ru_2^{5+} analogue, vide supra. The compound was structurally characterized.[125] The structural features of both $Os_2(chp)_4^+$ units are very similar and differ little from those of the dinuclear $Os_2(chp)_4Cl$. The complex has a magnetic moment (per Os_2 unit) that seems to be approaching a value appropriate for an $S = {}^3/_2$ state as the temperature rises, but it also falls rapidly, especially below 50 K, as though there is a significant coupling between the two Os_2 subunits through the bridging pyrazine ligand.

5.2. Squares

Molecular squares containing Ru_2^{5+} units, $[\{cis\text{-}Ru_2(\mu\text{-DAniF})_2Cl\}(\mu\text{-(LL)})]_4$, where LL = oxalate or terephthalate, have been prepared by reacting *cis*-$Ru_2(\mu\text{-DAniF})_2(\mu\text{-}O_2CCH_3)_2Cl$ with oxalic acid or terephthalic acid.[126] The *cis*-$Ru_2(\mu\text{-DAniF})_2(\mu\text{-}O_2CCH_3)_2$-Cl starting material was prepared by the reaction of $Ru_2(\mu\text{-}O_2CCH_3)_4Cl$ with 2.5 equiv of HAniF. The two squares have been structurally characterized and shown to have similar core structures that consist of four *cis*-$Ru_2(\mu\text{-DAniF})_2^{3+}$ units connected by dicarboxylate linkers forming square macrocycles. The Ru−Ru distances are 2.332(2) Å for the oxalate-containing square and 2.3323(7) Å and 2.347(7) Å for the terephthalate-containing square. These distances are very similar to that of 2.3192(3) Å in *cis*-$Ru_2(\mu\text{-DAniF})_2(\mu\text{-}O_2CCH_3)_2Cl$. The electrochemical behavior of the two squares was found to be somewhat complicated. CV measurements show that the two compounds exhibit reversible oxidation processes and less reversible reduction processes. DPV for the oxalate-containing square shows two oxidation waves at +1.052 V and +0.872 V and four reduction waves at −0.480 V, −0.700 V, and −0.836 V (two). DPV for the terephthalate shows two broad and slightly split signals centered at +0.804 V and −0.508 V. Due to the complexity of those redox processes, a precise estimate of the number of electrons involved cannot be obtained. However, these data are consistent with a higher degree of electronic communication between Ru_2^{5+} units in the oxalate-bridged species, due to the shorter length of the linker.

5.3. Polymers

Extended chains containing diruthenium(II,III) units, $[Ru_2(O_2CCH_3)_4(\mu\text{-L})]_\infty$, where L = $N(CN)_2^-$ or $C(CN)_3^-$, were prepared by reacting $[Ru_2(O_2CCH_3)_4(NCCH_3)_2][BF_4]$ with $NaN(CN)_2$ or $KC(CN)_3$.[124] Both compounds have been structurally characterized. In the compound with L = $N(CN)_2^-$, the dicyanamide ions bridge the $[Ru_2(O_2CCH_3)_4]^+$ units in an end-to-end bridging mode, thereby forming an alternating one-dimensional chain. In the compound with L = $C(CN)_3^-$, two cyano groups of the tricyanomethanide anion are coordinated to independent $[Ru_2(O_2CCH_3)_4]^+$ units to give a chain similar to that observed for the L = $N(CN)_2^-$ compound. The Ru−Ru distances in the $N(CN)_2^-$ and $C(CN)_3^-$ compounds are 2.2788(14) and 2.2756(5) Å, respectively, and are consistent with the values observed in $Ru_2(O_2CR)_4Cl$ and $[Ru_2(O_2CR)_4]^+$, which range from 2.27 to 2.29 Å. The temperature dependence of the magnetic susceptibility of the two compounds reveals a weak antiferromagnetic interaction between Ru_2 units ($S = {}^3/_2$) through each polycyano-anionic linker.

The reaction of $[Ru_2(O_2CC_2H_5)_4(H_2O)_2][BF_4]$ with phenazine yields the polymeric compound $[Ru_2(O_2CC_2H_5)_4(phz)][BF_4]$. The compound was structurally characterized. The phenazine ligands link the $[Ru_2(O_2CC_2H_5)_4]^+$ units into kinked chains.[127] The two crystallographically independent $[Ru_2(O_2CC_2H_5)_4]^+$ cations have Ru−Ru distances of 2.2756(6) and 2.2747(7) Å, respectively. These distances are typical of those found in $[Ru_2(O_2CR)_4]^+$ units. The BF_4^- ions

occupy general positions between the chains. The compound was shown to be antiferromagnetic with a magnetic moment of ca. 4.3 μ_B at 300 K that tends toward zero as 0 K is approached (1.72 μ_B at 2.7 K).

A compound with a 1D chain structure containing Ru_2^{5+} units, $[\{Na(THF)_2\}\{Ru_2(O_2CCH_3)_2(5\text{-Clsalpy})_2\}]\cdot THF$, was obtained upon the reaction of $Ru_2(O_2CCH_3)_4Cl$ with the tridentate ligand *N*-(2-pyridyl)-2-oxy-5-chlorobenzylaminate dianion (5-Clsalpy^{2-}).[128] The compound has been structurally characterized, and two formula units are included in the asymmetric unit. Each Ru_2 unit is composed of two bridging acetate groups and two 5-Clsalpy^{2-} groups, forming the anionic Ru_2(II,III) unit, $[Ru_2(O_2CCH_3)_2(5\text{-Clsalpy})_2]^-$. The Ru−Ru distances of 2.2949(5) and 2.2898(5) Å are very close to those observed in $Ru_2(O_2CR)_4Cl$ and $[Ru_2(O_2CR)_4]^+$. The Na^+ counterions are surrounded by the phenolate oxygen atoms with the support of two THF molecules, and form an alternating chain. The CV of the compound shows one reduction and three oxidations observed as quasi-reversible waves. The one-electron reduction was assigned to the metal-centered $Ru_2^{II,III}/Ru_2^{II,II}$ couple, and the first and second oxidations were assigned to the metal-centered $Ru_2^{III,III}/Ru_2^{II,III}$ and $Ru_2^{III,IV}/Ru_2^{III,III}$ couples, respectively. The third couple is achieved by the two-electron oxidation, which arises from 5-Clsalpy^{2-}-centered oxidations.

6. M_2 Starting Materials with a Bond Order of 2

Complexes containing MM double bonds are much rarer than those having quadruple or triple bonds, and so it is not surprising to find such limited examples as those described below.

6.1. Clusters

The compounds $W_4(OR)_{16}$ where R = Me,[129] Et,[130] and ^{n}Pr[131] are the only known cluster compounds that can reasonably be viewed as the product of the coupling of two $(W{=}W)^{8+}$ units. These compounds arise from the oxidative addition to the W≡W bond in reactions involving $W_2(NMe_2)_6$ and the respective alcohol. The exact course of the reaction is not known, although likely intermediates of the type $W_2(\mu\text{-H})(OR)_7L$, which are known for R = ^{i}Pr[132] and $CH_2{}^t$Bu,[133] where L = a Lewis base such as an amine or PMe_3, are involved. The molecular structure of the *n*-propoxide was recently determined, and in the solid state, there were two independent molecules in the unit cell.[131] These structures are essentially the same as that originally reported for $W_4(OEt)_{16}$, which is shown in Figure 36. The W_4O_{16} unit is centrosymmetric, and the four tungsten atoms form a rhombus with two short edges, W(1)−W(2) and W(1)′−W(2)′, and two long edges, W(1)′−W(2) and W(2)′−W(1), of distances ca. 2.6 and 2.9 Å, respectively. The backbone W(1)−W(1)′ distance of ca. 2.75 Å is intermediate and clearly a MM bonding distance. There are two μ_3-OR groups, one above and one below the W_4 plane, and four edge-bridging OR groups (μ_2-OR). The outer tungstens have three terminal OR groups while the backbone tungstens have two. Each tungsten atom is in a pseudo-octahedral environment. The bonding in these unusual clusters was originally

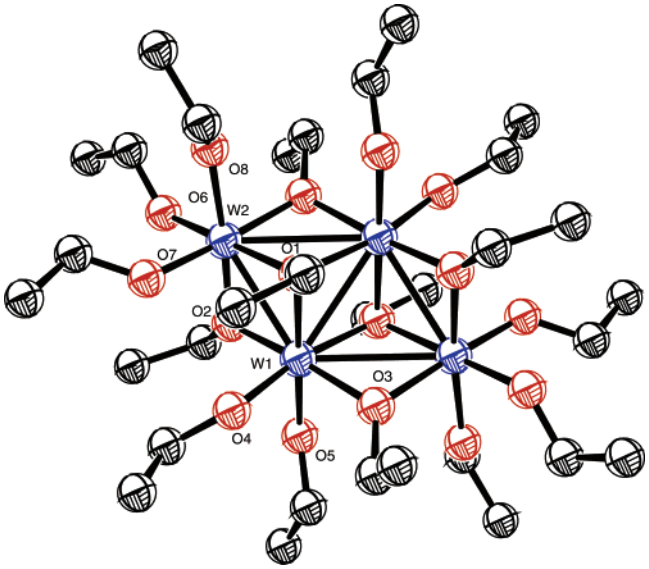

Figure 36. Molecular structure of the centrosymmetric $W_4(OEt)_{16}$ cluster. Hydrogen atoms are omitted for clarity, and only one set of symmetry-equivalent tungsten and oxygen atoms is labeled.

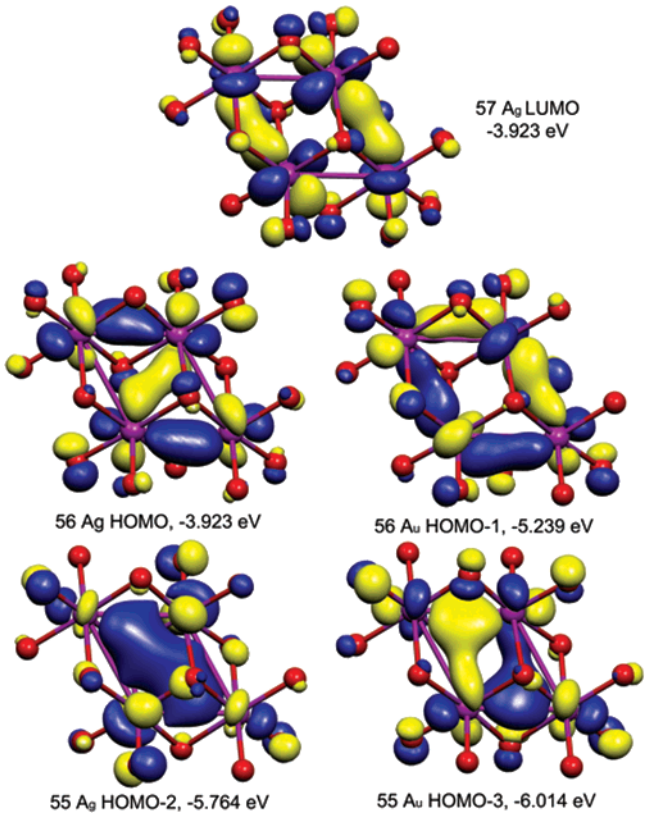

Figure 37. Calculated molecular orbitals for $W_4(OH)_{16}$. Geometry optimization and electronic structure calculations on this molecule were carried out using ADF 2004.01 using C_i symmetry restraints.

examined by Cotton and Fang, who employed the model compound $Mo_4(OH)_{16}$ and the methods of Fenske and Hall.[134] More recently, DFT calculations using the Amsterdam Density Functional 2004.1 package were applied to the model compound $W_4(OH)_{16}$ in C_i symmetry.[135] Plots of the frontier molecular orbitals for the model compound $W_4(OH)_{16}$ are given in Figure 37. The HOMO, HOMO-1,

HOMO-2, and HOMO-3 all have metal−metal bonding character, as does the LUMO. Indeed, population of the LUMO would be expected to generate a 10-electron M_4 cluster with nearly equal M−M distances.

^{1}H and ^{13}C{^{1}H} NMR studies revealed that the $W_4(OR)_{16}$ compounds are rigid on the NMR time scale and do not undergo rapid bridge−terminal alkoxide site exchange. There are, in fact, eight nonequivalent OR groups of equal integral intensity, as predicted by solid-state structures.[129]

6.2. Dimers of "Dimers"

The compound $W_4(H)_2(O^iPr)_{14}$ is a black, crystalline, hydrocarbon-soluble material formed in the reaction between $W_2(NMe_2)_6$ and excess ^{i}PrOH.[136] This compound was crystallographically characterized and found to contain a four-atom chain of tungsten atoms with short, 2.45 Å, long, 3.3 Å, and short, 2.45 Å, WW distances corresponding to WW double (2.45 Å) and nonbonding (3.3 Å) distances. In solution, the compound is fluxional, and only one type of O^{i}Pr group is observed by ^{1}H NMR. Evidently, here, bridge−terminal alkoxide−site exchange is rapid. Rather interestingly, the hydride signal occurs downfield at δ 7.96 and shows coupling to two equivalent ^{183}W nuclei (^{183}W, $I = {}^1/_2$, 14.5 natural abundance), $J(^{183}W-^1H) = 95$ Hz. This compound can be cleaved to form $W_2(H)(O^iPr)_8L$ adducts with L = pyridine or PMe_3, and a related adduct, $NaW_2(H)(O^iPr)_8$·diglyme, was crystallographically characterized, as was a similar neopentoxide, $W_2(H)(I)(OCH_2{}^tBu)_6$·H_2NMe.[137]

The compounds $W_2(O^tBu)_6(\mu$-CO) and $W_2(O^iPr)_6(py)_2(\mu$-CO) may be considered to have MM double bonds and be inorganic analogues of cyclopropenones.[138,139] The W−W distances are ca. 2.45 Å, and the ν(CO) values are in the range 1575−1600 cm^{-1}, indicative of extensive W_2 dπ to CO π^* back-bonding. In solution, the compound $W_2(O^iPr)_6(py)_2(\mu$-CO) loses pyridine to dimerize to form $[W_2(O^iPr)_6(py)(\mu$-CO)]$_2$,[139] and the compound $W_2(O^tBu)_6(\mu$-CO) reacts with ^{i}PrOH to give $[W_2(O^iPr)_6(\mu$-CO)]$_2$.[138] Most interestingly, in these tetranuclear carbonyl compounds, it is the CO ligand that is involved in the formation of the dimers of "dimers" as shown in Figure 38. Upon dimerization of the $W_2(OR)_6(\mu$-CO) unit, the W−W bond lengthens to 2.65 Å, the W−C bond distances decrease, 1.95 Å, the C−O bond lengthens (to 1.34 Å), and the W−O bond distance to the carbonyl ligand is 1.96 Å, comparable to that of a W−O alkoxide bond. Collectively, these structural changes indicate the further reduction of the CO ligand as a result of W_2 dπ to CO π^* bonding and CO pπ to W dπ donation.

A series of complexes in which edge-sharing bioctahedral dirhenium units are linked by $[N(CN)_2]^-$, $[C(CN)_3]^-$, and $[Ni(CN)_4]^{2-}$ ions has been prepared. This series includes the following compounds: $\{[Re_2Cl_3(\mu$-dppm$)_2(CO)_2]_2[\mu$-N(CN)$_2]\}$Cl, $\{[Re_2Cl_3(\mu$-dppm$)_2(CO)_2]_2[\mu$-C(CN)$_3]\}$Cl, $[Re_2Cl_3(\mu$-dppe$)_2(CO)_2]_2[\mu$-Ni(CN)$_4]$ (dppe = 1,2-bis(diphenylphosphine)-ethylene), $[Re_2Cl_3(\mu$-dppm$)_2(CO)_2]_2[\mu$-Ni(CN)$_4]$, $[Re_2Cl_3(\mu$-dppm$)_2(CO)(CNXyl)]_2[\mu$-Ni(CN)$_4]$. Two of these complexes, $\{[Re_2Cl_3(\mu$-dppm$)_2(CO)_2]_2[\mu$-N(CN)$_2]\}$Cl and $[Re_2Cl_3(\mu$-dppe$)_2(CO)_2]_2[\mu$-Ni(CN)$_4]$, have been structurally characterized;[140] the Re−Re distances were found to be ca. 2.58 Å, which is consistent with the presence of a Re=Re double bond. Three of the complexes, $\{[Re_2Cl_3(\mu$-dppm$)_2(CO)_2]_2[\mu$-N(CN)$_2]\}$Cl, $\{[Re_2Cl_3(\mu$-dppm$)_2(CO)_2]_2[\mu$-C(CN)$_3]\}$Cl, and $[Re_2Cl_3(\mu$-dppm$)_2(CO)(CNXyl)]_2[\mu$-Ni(CN)$_4]$, were sufficiently soluble to obtain cyclic voltammetric data. All three complexes show the presence of pairs of sequential one-electron redox processes for $E_{1/2}$(ox.) and $E_{1/2}$(red.), although, in the case of $[Re_2Cl_3(\mu$-dppe$)_2(CO)_2]_2[\mu$-Ni(CN)$_4]$, the pair processes for the reduction were not resolved. The values of K_c for $\{[Re_2Cl_3(\mu$-dppm$)_2(CO)_2]_2[\mu$-N(CN)$_2]\}$Cl were 1.10×10^3 and 115 for oxidation and reduction, respectively. For $\{[Re_2Cl_3(\mu$-dppm$)_2(CO)_2]_2[\mu$-C(CN)$_3]\}$Cl, the values of K_c were 2.49×10^4 (ox.) and 1.10×10^3 (red.), and for $[Re_2Cl_3(\mu$-dppm$)_2(CO)(CNXyl)]_2[\mu$-Ni(CN)$_4]$, the K_c for the oxidation is 506.[140]

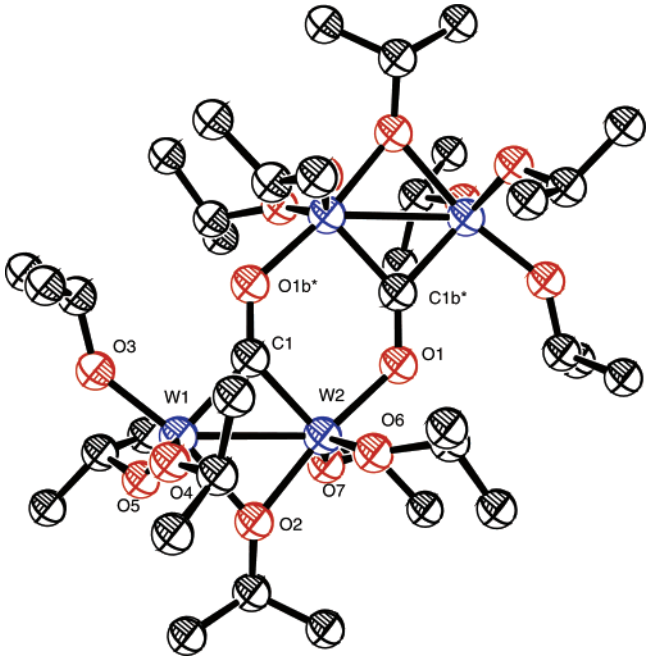

Figure 38. Molecular structure of $W_4(\mu_3$-η^1,η^2-CO$)_2$-$(O^iPr)_{12}$. Alkoxide hydrogen atoms are omitted, and one set of tungsten atoms is labeled along with the carbon and oxygen atoms of the μ_3-CO ligands.

A mixed-metal assembly, $[Re_2Cl_3(\mu$-dppe$)_2(CO)_2(\mu$-NCS$)]_2Pd_2(\mu$-SCN$)(\mu$-NCS$)Cl_2$, in which two Re_2^{4+}-containing cations, $[Re_2Cl_3(\mu$-dppe$)_2(CO)_2]^+$, are linked by a $[Pd_2(\mu$-SCN$)(\mu$-NCS$)Cl_2(SCN)_2]^{2-}$ anion has been prepared by Walton and co-workers.[141,142] The complex was prepared by the addition of NaSCN to a solution containing $[Re_2Cl_3(\mu$-dppe$)_2(CO)_2]^+$ and Pd(1,5-COD)Cl_2. The complex has been characterized crystallographically.[141] The Re−Re bond distance of 2.5775(4) Å indicates that the Re=Re double bond present in the starting material is retained. Two different types of bridging thiocyanato ligands are present, which resulted in two different Pd−S bond lengths. The Pd−S bond lengths were found to be very similar, 2.333(3) and 2.325(3) Å.

6.3. Chains

The compound WCl_4 has recently been prepared and characterized by Messerle and shown to exist in the solid state as an extended chain structure of edge-bridged tungsten octahedra depicted in **VI** below.[143] The alternation of short, 2.69 Å, and long, 3.79 Å, WW distances can reasonably be assigned to localized d^2-d^2 MM double bonds and nonbonding distances, respectively.

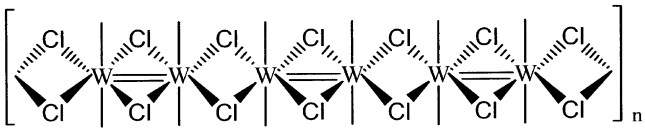

VI

The compound $[W_2(OCH_2{}^tBu)_8]$[144] also exists in the solid state as a polymer and, on the basis of analogy with the UV−vis spectroscopic properties of the structurally characterized compound $W_2(OCH_2{}^tBu)_8(py)$,[145] is believed to contain alkoxide-bridged face-sharing octahedra.

Another example of MM double bonds in a solid-state extended lattice structure can be seen for MoO_2, which adopts a distorted rutile structure with short and long Mo−Mo distances.[146]

The ruthenium trifluoroacetate complex $Ru_2(O_2CCF_3)_4$ has an electron-rich MM double bond of configuration $\sigma^2\pi^4\delta^2\delta^{*2}\pi^{*2}$ and binds ligands in the axial position. With phenazine (phz), it forms a one-dimensional polymer of the formula $[Ru_2(O_2CCF_3)_4(phz)]_n$ as shown in Figure 39.[147] From magnetic

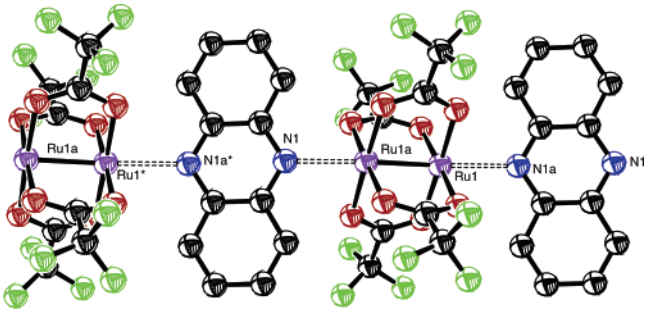

Figure 39. Extended molecular structure of $Ru_2[O_2CCF_3]_4$·(phz). The Ru−Ru−N−N−Ru−Ru−N−N atoms involved in the intermolecular interactions are labeled, and the Ru−N interactions are highlighted using dashed bonds. The hydrogen atoms on the phz ligands are omitted for clarity.

susceptibility data, it was shown that the Ru_2^{4+} centers are only very weakly antiferromagnetically coupled through the phenazine bridge. Other $Ru_2(O_2CR)_4$ compounds, particularly those with long alkyl chains, have been shown to form 1:1 adducts with pyrazine in the solid state and also shown to maintain some degree of oligomerization in solution.[148]

The $Ru_2(O_2CCF_3)_4$ molecule has also been shown to form a network sheet structure with TCNQ, $[Ru_2O_2(CCF_3)_4]_2(\mu_4\text{-TCNQ})$. The slightly longer Ru−Ru distance in this network solid relative to that in $Ru_2(O_2CCF_3)_4$·2THF, together with the reduction in the values of ν(CN) relative to those for free TCNQ, provided evidence for metal−TCNQ π donation.[149]

7. Acknowledgment

We thank the National Science Foundation for support of this work (NSF CHE-0131832) and Carl "Burt" Hollandsworth for preparation of the figures. A.M.M. would like to thank the KY NSF EPSCoR program and the Commonwealth of Kentucky for continued research support.

8. References

(1) DeKock, R. L.; Gray, H. B. *Chemical Structure and Bonding*; University Science Books: Mill Valley, CA, 1989.
(2) Cotton, F. A.; Curtis, N. F.; Harris, C. B.; Johnson, B. F. G.; Lippard, S. J.; Mague, J. T.; Robinson, W. R.; Wood, J. S. *Science* **1964**, *145*, 1305.
(3) Cotton, F. A.; Walton, R. A. *Multiple Bonds Between Metal Atoms*, 2nd ed.; Oxford University Press: Oxford, U.K., 1993.
(4) (a) Pelin, M. J.; Foosnces, T.; Gruen, D. M. *J. Chem. Phys.* **1981**, *74*, 5547. (b) Bursten, B. E.; Cotton, F. A.; Hall, M. B. *J. Am. Chem. Soc.* **1980**, *102*, 6349. (c) Atha, P. M.; Hillier, I. H.; Guest, M. F. *Chem. Phys. Lett.* **1980**, *75*, 84.
(5) Chisholm, M. H.; Extine, M. W.; Kelly, R. L.; Mills, W. C.; Murrillo, C. A.; Rankel, L. A.; Reichert, W. W. *Inorg. Chem.* **1978**, *17*, 1673.
(6) McGinnis, R. N.; Ryan, T. R.; McCarley, R. E. *J. Am. Chem. Soc.* **1978**, *100*, 7900.
(7) Cotton, F. A.; Shang, M. *J Cluster Sci.* **1991**, *2*, 121.
(8) Ryan, T. R.; McCarley, R. E. *Inorg. Chem.* **1982**, *21*, 2072.
(9) Cotton, F. A.; Powell, G. L. *Inorg. Chem.* **1983**, *22*, 871.
(10) Cotton, F. A.; Hong, B.; Shang, M. *Inorg. Chem.* **1993**, *32*, 4876.
(11) McCarley, R. E.; Rayan, T. R.; Torardi, C. C. *Am. Chem. Soc. Symp. Ser. No. 155*, 41.
(12) Carlin, R. T.; McCarley, R. E. *Inorg. Chem.* **1989**, *28*, 3432.
(13) Shrock, R. R.; Strurgeoff, L. G.; Sharp, P. R. *Inorg. Chem.* **1983**, *22*, 2801.
(14) Beers, W. W.; McCarley, R. E. *Inorg. Chem.* **1985**, *24*, 468.
(15) Beers, W. W.; McCarley, R. E. *Inorg. Chem.* **1985**, *24*, 472.
(16) Chen, J.-D.; Cotton, F. A. *J. Am. Chem. Soc.* **1991**, *113*, 5857.
(17) Cotton, F. A.; Dikarev, E. V. *J. Cluster Sci.* **1995**, 6, 411.
(18) Lau, S. S.; Fanwick, P. E.; Walton, R. A. *Dalton Trans.* **1999**, 2273.
(19) Bera, J. K.; Lau, S. S.; Fanwick, P. E.; Walton R. A. *J. Chem. Soc., Dalton Trans.* **2000**, 4277.
(20) Cotton, F. A.; Daniels, L. M.; Guimet, I.; Henning, R. W.; Jordan, G. T., IV.; Lin, C. Murrilllo, C. A.; Schultz, A. J. *J. Am. Chem. Soc.* **1998**, *120*, 12531.
(21) Cotton, F. A.; Liu, C. Y.; Murillo, C. A.; Wang, X. *Chem. Commun.* **2003**, 2190.
(22) Cotton, F. A.; Daniels, L. M.; Jordan, G. T., IV.; Lin, C.; Murillo, C. A. *J. Am. Chem. Soc.* **1998**, *120*, 3398.
(23) Cotton, F. A.; Daniels, L. M.; Jordan, G. T., IV.; Lin, C.; Murillo, C. A. *Inorg. Chem. Commun.* **1998**, *1*, 109.
(24) Cayton, R. H.; Chisholm, M. H.; *J. Am. Chem. Soc.* **1989**, *111*, 8921.
(25) Cayton, R. H.; Chisholm, M. H.; Huffman, J. C.; Lobkovsky, E. B. *Angew. Chem., Int. Ed. Engl.* **1991**, *30*, 862.
(26) Cayton, R. H.; Chisholm, M. H.; Huffman, J. C.; Lobkovsky, E. B. *J. Am. Chem. Soc.* **1991**, *113*, 8709.
(27) Chisholm, M. H. *Dalton Trans.* **2003**, 3821.
(28) Chisholm, M. H. *J. Organomet. Chem.* **2002**, *641*, 15.
(29) Bursten, B. E.; Chisholm, M. H.; Hadad, C. M.; Li, J.; Wilson, P. J. *Chem Commun.* **2001**, 2382.
(30) Bursten, B. E.; Chisholm, M. H.; Clark, R. J. H.; Firth, S.; Hadad, C. M.; Macintosh, A. M.; Wilson, P. J.; Woodward, P. M.; Zaleski, J. M. *J. Am. Chem. Soc.* **2002**, *124*, 3050.
(31) Bursten, B. E.; Chisholm, M. H.; Hadad, C. M.; Li, J.; Wilson, P. J. *Isr. J. Chem.* **2002**, *41*, 187.
(32) Byrnes, M. J.; Chisholm, M. H.; Dye, D. F.; Hadad, C. M. Pate, B. D.; Wilson, P. J.; Zaleski, J. M. *Dalton Trans.* **2004**, 523.
(33) Bursten, B. E.; Chisholm, M. H.; Clark, R. J. H.; Firth, S.; Hadad, C. M.; Wilson, P. J.; Woodward, P. M.; Zaleski, J. M. *J. Am. Chem. Soc.* **2002**, *124*, 12244.
(34) Byrnes, M. J.; Chisholm, M. H. *Chem. Commun.* **2002**, 2040.
(35) Cotton, F. A.; Donahue, J. P.; Murillo, C. A. *J. Am. Chem. Soc.* **2003**, *125*, 5436.
(36) Cotton, F. A.; Donahue, J. P.; Murillo, C. A.; Perez, L. M. *J. Am. Chem. Soc.* **2003**, *125*, 5486.
(37) Cotton, F. A.; Lin, C.; Murillo, C. A. *J. Chem. Soc., Dalton Trans.* **1998**, 3151.

(38) Cotton, F. A.; Donahue, J. P.; Lin, C.; Murillo, C. A. *Inorg. Chem*. **2001**, *40*, 1234.
(39) Cotton, F. A.; Donahue, J. P.; Murillo, C. A. *Inorg. Chem. Commun*. **2002**, *5*, 59.
(40) Cotton, F. A.; Donahue, J. P.; Lin, C. Murillo, C. A.; Rockwell, J. *Acta Crystallogr.* **2002**, *E58*, m298.
(41) Chisholm, M. H.; Macintosh, A. M. *J. Chem. Soc., Dalton Trans*. **1999**, 1205.
(42) Richardson, D. E.; Taube, H. *Inorg. Chem*. **1981**, *20*, 1278.
(43) Robin, M. B.; Day, P. *Adv. Inorg. Chem. Radiochem*. **1967**, *10*, 247.
(44) Chisholm, M. H.; Pate, B. D.; Wilson, P. J.; Zaleski, J. M. *Chem. Commun*. **2002**, 1084.
(45) Chisholm, M. H.; Feil, F. Results to be published.
(46) Cotton, F. A.; Donahue, J. P.; Murillo, C. A.; Perez, L. M.; Yu, R. *J. Am. Chem. Soc.* **2003**, *125*, 8900.
(47) Chisholm, M. H.; Clark, R. J. H.; Hadad, C. M.; Patmore, N. J. *Chem. Commun*. **2004**, 80.
(48) Chisholm, M. H.; Clark, R. J. H.; Gallucci, J.; Hadad, C. M.; Patmore. N. J. *J. Am. Chem. Soc.* **2004**, *126*, 8303.
(49) Cayton, R. H.; Chisholm, M. H.; Putilina, E. F.; Folting, K. *Polyhedron* **1993**, *12*, 2627.
(50) Cotton, F. A.; Donahue, J. R.; Liu, C. Y.; Murillo, C. A. *Inorg. Chem.* **2002**, *41*, 1354.
(51) Cotton, F. A.; Liu, C. Y.; Murillo, C. A.; Villagran, D.; Wang, X. *J. Am. Chem. Soc.* **2003**, *125*, 13564.
(52) Cotton, F. A.; Donahue, J. P.; Murillo, C. A. *Inorg. Chem*. **2001**, *40*, 2229.
(53) Cotton, F. A.; Liu, C. Y.; Murillo, C. A.; Wang, X. *Inorg. Chem*. **2003**, *42*, 4619.
(54) Cotton, F. A.; Dalal. N. S.; Liu, C. Y.; Murillo, C. A.; North, J. M.; Wang, X. *J. Am. Chem. Soc.* **2003**, *125*, 12945.
(55) Mashima, K.; Nakano, H.; Nakamura, A. *J. Am. Chem. Soc.* **1993**, *115*, 11632.
(56) Nakano, H.; Nakamura, A.; Mashima, K. *Inorg. Chem.* **1996**, *35*, 4007.
(57) Cayton, R. H.; Chisholm, M. H.; Putilina, E. F.; Folting, K.; Huffman, J. C.; Moodley, K. G. *Inorg. Chem.* **1992**, *31*, 2928.
(58) Bakir, M.; Walton, R. A. *Polyhedron* **1987**, *6*, 1925.
(59) Cotton, F. A.; Lu, J. Huang, Y. *Inorg. Chem*. **1996**, *35*, 1839.
(60) Cotton, F. A.; Dikarev, E. V.; Petrukhina, M. A. *Inorg. Chim. Acta* **2002**, *334*, 67.
(61) Ding, Y.; Lau, S. S.; Fanwick, P. E.; Walton, R. A. *Inorg. Chim. Acta* **2000**, *300*−*302*, 505.
(62) Whelan, E.; Devereux, M.; McCann, M.; McKee, V. *Chem. Commun*. **1997**, 427.
(63) Cotton, F. A.; Lin, C.; Murillo, C. A. *Inorg. Chem*. **2001**, *40*, 472.
(64) Berry, J. F.; Cotton, F. A.; Ibragimov, S. A.; Murillo, C. A.; Wang, X. *Dalton Trans.* **2003**, 4297.
(65) Cotton, F. A.; Daniels, L. M.; Lin, C.; Murillo, C. A. *J. Am. Chem. Soc*. **1999**, *121*, 4538.
(66) Cotton, F. A.; Lin, C.; Murillo, C. A. *Inorg. Chem*. **2001**, *40*, 478.
(67) Cotton, F. A.; Lin, C.; Murillo, C. A. *Inorg. Chem*. **2001**, *40*, 575.
(68) (a) Cotton, F. A.; Lin, C.; Murillo, C. A. *Proc. Natl. Acad. Sci.* **2002**, *99*, 4810. (b) Cotton, F. A.; Lin, C.; Murillo, C. A. *Acc. Chem. Res*. **2001**, *34*, 759.
(69) Cotton, F. A.; Daniels, L. M.; Lin, C.; Murillo, C. A. *Chem. Commun*. **1999**, 841.
(70) Cotton, F. A.; Lin, C.; Murillo, C. A. *Inorg. Chem*. **2001**, *40*, 6413.
(71) Suen, M.-C.; Tsen, G.-W.; Chen, J.-D.; Keng, T.-C.; Wang, J.-C. *Chem. Commun.* **1999**, 1185.
(72) Cotton, F. A.; Lin, C.; Murillo, C. A. *J. Am. Chem. Soc.* **2001**, *123*, 2670.
(73) Cotton, F. A.; Daniels, L. M.; Murillo, C. A.; Wang, X. *Chem. Commun*. **1998**, 39.
(74) Cotton, F. A.; Daniels, L. M.; Lu, T.; Murillo, C. A.; Wang, X. *J. Chem. Soc., Dalton Trans.* **1999**, 517.
(75) Day, E. F.; Huffman, J. C.; Folting, K.; Christou, G. *J. Chem. Soc., Dalton Trans.* **1997**, 2837.
(76) Handa, M.; Kasamatsu, K.; Kasuga, K.; Mikuriya, M.; Fujii, T. *Chem. Lett.* **1990**, 1753.
(77) Handa, M.; Mikuriya, M.; Katera, T.: Yamada, K.; Nakao, T.; Matsumada, H.; Kasuga, K. *Bull. Chem. Soc. Jpn.* **1995**, *68*, 2567.
(78) Handa, M.; Yamada, K.; Nakao, T.; Kasuga, K.; Mikuriya, M.; Kotera, T. *Bull. Chem. Soc. Jpn.* **1994**, *67*, 3125
(79) Handa, M.; Yamada, K.; Nakao, T.; Kasuga, K.; Mikuriya, M.; Kotera, T. *Chem. Lett*. **1993**, 1969.
(80) Handa, M.; Matsumoto, H.; Yoshieka, D.; Nukada, R.; Mikuriya, M.; Hirmitsu, I.; Kasuga, K. *Bull. Chem. Soc. Jpn.* **1998**, *71*, 1811.
(81) Handa, M.; Sono, H.; Kasamatsu, K.; Kasuga, K.; Mikuriya, M.; Ikenoue, S. *Chem. Lett*. **1992**, 453.
(82) Kerby, M. C.; Eichhorn, B. W.; Creighton. J. A.; Vollhardt, P. C. *Inorg. Chem.* **1990**, *29*, 1319.
(83) Eichhorn, B. W.; Kerby, M. C.; Ahmed, K. J.; Huffman, J. C. *Polyhedron* **1991**, *10*, 2573.
(84) Campana, C.; Dunbar, K. R.; Ouyang, X. *Chem. Commun*. **1996**, 2427.
(85) Ouyang, X.; Campana, C.; Dunbar, K. R.; *Inorg. Chem.* **1996**, *35*, 7188.
(86) Kuang, S.-M.; Fanwick, P. E.; Walton, R. A. *Inorg. Chem. Commun*. **2002**, *5*, 13.
(87) Cotton, F. A.; Felthouse, T. R. *Inorg. Chem.* **1980**, *19*, 328.
(88) Osmanov, N. S.; Kotel′nikova, A. S.; Koz′min, P. A.; Abbasova, T. A.; Surazhskaya, M. D.; Larina, T. B. *Russ. J. Inorg. Chem.* **1988**, *33*, 457.
(89) Bera, J. K.; Vo, T.-T.; Walton, R. A.; Dunbar, K. R. *Polyhedron* **2003**, *22*, 3009.
(90) Kuang, S.-M.; Fanwick, P. E.; Walton, R. A. *Inorg. Chem. Commun.* **2001**, *4*, 745.
(91) Kung, S.-M.; Fanwick, P. E.; Walton, R. A. *Inorg. Chem.* **2002**, *41*, 405.
(92) Bera, J. K.; Angardidis, P.; Cotton, F. A.; Petrukhina, M. A.; Fanwick, P. E.; Walton, R. A. *J. Am. Chem. Soc.* **2001**, *123*, 1515.
(93) Bera, J. K.; Clerac, R.; Fanwick. P. E.; Walton, R. A. *J. Chem. Soc., Dalton Trans*. **2002**, 2168.
(94) Chisholm, M. H.; Clark, D. L.; Folting, K.; Huffman, J. C. *Angew. Chem., Int. Ed. Engl.* **1986**, *25*, 1014.
(95) Chisholm, M. H.; Clark, D. L.; Folting, K.; Huffman, J. C.; Hampden-Smith, M. *J. Am. Chem. Soc.* **1987**, *109*, 7750.
(96) Chisholm, M. H.; Folting, K.; Hammond, C. E.; Hampden-Smith, M. J. *J. Am. Chem. Soc.* **1988**, *110*, 3314.
(97) Chisholm, M. H.; Folting, K.; Hammond, C. E.; Hampden-Smith, M. J.; Moodley, K. G. *J. Am. Chem. Soc.* **1989**, *111*, 5300.
(98) Chisholm, M. H.; Clark, D. L.; Hampden-Smith, M. J. *J. Am. Chem. Soc.* **1989**, *111*, 574.
(99) Chisholm, M. H.; Errington, R. J.; Folting, K.; Huffman, J. C. *J. Am. Chem. Soc.* **1982**, *104*, 2025.
(100) Chisholm, M. H.; Clark, D. L.; Errington, R. J.; Folting, K.; Huffman, J. C. *Inorg. Chem.* **1988**, *27*, 2071.
(101) Bursten, B. E.; Chisholm, M. H.; Clark, D. L. *Inorg. Chem.* **1988**, *27*, 2084.
(102) Chisholm, M. H.; Folting, K.; Eichhorn, B. W.; Huffman, J. C. *J. Am. Chem. Soc.* **1987**, *109*, 3146.
(103) Chisholm, M. H.; Folting, K.; Hammond, C. E.; Huffman, J. C.; Martin, J. D. *Angew. Chem., Intl. Ed. Engl.* **1989**, *28*, 1368.
(104) Chisholm, M. H.; Hammond, C. E.; Huffman, J. C.; Martin, J. D. *Polyhedron* **1990**, *9*, 1829.
(105) Budzichowski, T. A.; Chisholm, M. H.; Huffman, J. C.; Kramer, K. S.; Eisenstein, O. *J. Chem. Soc., Dalton Trans.* **1998**, 2563.
(106) Budzichowski, T. A.; Chisholm, M. H.; Huffman, J. C.; Eisenstein, O. *Angew. Chem., Int. Ed. Engl.* **1994**, *33*, 191.
(107) Chisholm, M. H.; Folting, K.; Kramer, K. S.; Streib, W. E. *J. Am. Chem. Soc.* **1997**, *119*, 5528.
(108) Chisholm, M. H.; Kramer, K. S.; Streib, W. E. *J. Am. Chem. Soc.* **1992**, *114*, 3571; correction *J. Am. Chem. Soc.* **1995**, *117*, 6152.
(109) Chisholm, M. H.; Kramer, K. S. *Chem. Commun.* **1996**, 1331.
(110) Chisholm, M. H.; Huffman, J. C.; Kramer, K. S.; Streib, W. E. *J. Am. Chem. Soc.* **1993**, *115*, 9866.
(111) Chisholm, M. H.; Hammond, C. E.; Hampden-Smith, M.; Huffman, J. C.; Van Der Sluys, W. G. *Angew. Chem., Int. Ed. Engl.* **1987**, *26*, 904.
(112) Chisholm, M. H.; Huffman, J. C.; Kelly, R. L. *J. Am. Chem. Soc.* **1979**, *101*, 7100.
(113) Chisholm, M. H.; Clark, D. L.; Huffman, J. C. *Polyhedron* **1985**, *4*, 1203.
(114) Chisholm, M. H.; Click, D. R.; Huffman, J. C. *J. Organomet. Chem.* **2000**, *614*−*615*, 238.
(115) Chisholm, M. H.; Gallucci, J. C.; Hollandsworth, C. B. *J. Organomet. Chem.* **2003**, *684*, 269.
(116) Bartley, S. L.; Dunbar, K. R. *Angew. Chem., Int. Ed. Engl.* **1991**, *30*, 448.
(117) Cotton, F. A.; Vidyasagar, K. *Inorg. Chim. Acta* **1989**, *166*, 109.
(118) Bera, J. K.; Smucker, B. W.; Walton, R. A.; Dunbar, K. R. *Chem. Commun*. **2001**, 2562.
(119) Bera, J. K.; Bacsa, J.; Smucker, B. W.; Dunbar, K. R. *Eur. J. Inorg. Chem*. **2004**, 368.
(120) Cotton, F. A.; Kim, Y.; Ren, T. *Inorg. Chem.* **1992**, *31*, 2608.
(121) Angaridis, P.; Berry, J. F.; Cotton, F. A.; Lei, P.; Chun, L.; Murillo, C. A.; Villagran, D. *Inorg. Chem. Commun.* **2004**, *7*, 9.
(122) Ren, T.; Zou, G.; Alvarez, J. C. *Chem. Commun.* **2000**, 1197.
(123) Hurst, S. K.; Ren, T. *J. Organomet. Chem.* **2002**, *660*, 1.
(124) Miyaska, H.; Clerac, R.; Campos-Fernandez, C. S.; Dunbar, K. R. *Inorg. Chem.* **2001**, *40*, 1663.
(125) Cotton, F. A.; Kim, Y.; Schultz, D. L. *Inorg. Chim. Acta* **1995**, *236*, 43.
(126) Angardidis, P.; Berry, J. F.; Cotton, F. A.; Murillo, C. A.; Wang, X. *J. Am. Chem. Soc.* **2003**, *125*, 10327.
(127) Cotton, F. A.; Kim, Y.; Ren, T. *Inorg. Chem.* **1992**, *31*, 2723.
(128) Miyasaka, H.; Kachi-Terajima, C.; Ishii, T.; Yamashita, M. *J. Chem. Soc., Dalton Trans.* **2001**, 1929.
(129) Chisholm, M. H.; Huffman, J. C.; Kirkpatrick, C. C.; Leonelli, J. Folting, K. *J. Am. Chem. Soc.* **1981**, *103*, 6093.
(130) Chisholm, M. H.; Huffman, J. C.; Leonelli, J. *J. Chem. Soc., Chem. Commun*. **1981**, 270.
(131) Chisholm, M. H.; Galluchi, J. C.; Hollandsworth, C. B. Results to be published.

(132) Akiyama, M.; Chisholm, M. H.; Cotton, F. A.; Extine, M. W.; Haitko, D. A.; Leonelli, J.; Little, D. *J. Am. Chem. Soc.* **1981**, *103*, 779.
(133) Barry, J. T.; Chacon, S. T.; Chisholm, M. H.; Huffman, J. C.; Streib, W. E. *J. Am. Chem. Soc.* **1995**, *117*, 1974.
(134) Cotton, F. A.; Fang, A. *J. Am. Chem. Soc.* **1982**, *104*, 113.
(135) Chisholm, M. H.; Hollandsworth, C. B. Results to be published.
(136) Akiyama, M.; Little, D.; Chisholm, M. H.; Haitko, D. A.; Cotton, F. A.; Extine, M. W. *J. Am. Chem. Soc.* **1979**, *101*, 2504.
(137) Chisholm, M. H.; Huffman, J. C.; Smith, C. A. *J. Am. Chem. Soc.* **1986**, *108*, 222.
(138) Chisholm, M. H.; Hoffman, D. M.; Huffman, J. C. *Organometallics* **1985**, *4*, 986.
(139) Cotton, F. A.; Schwotzer, W. *J. Am. Chem. Soc.* **1983**, *105*, 4955.
(140) Kuang, S.-M.; Fanwick, P. E.; Walton, R. A. *Inorg. Chem.* **2002**, *41*, 147.
(141) Kuang, S.-M.; Fanwick, P. E.; Walton, R. A. *Inorg. Chem.* **2000**, *39*, 2968.
(142) Kuang, S.-M.; Fanwick, P. E.; *Inorg. Chem.* **2001**, *40*, 5682.
(143) Kolesnichenko, V.; Swenson, D. C.; Messerle, L. *Inorg. Chem.* **1998**, *37*, 3257.
(144) Chisholm, M. H.; Streib, W. E.; Tiedtke, D. B.; Wu, D.-D. *Chem.—Eur. J.* **1998**, *4*, 1470.
(145) Budzichowski, T. A.; Chisholm, M. H.; Folting, K. Huffman, J. C.; Streib, W. E. *J. Am. Chem. Soc.* **1995**, *117*, 7428.
(146) Brandt, B. G.; Skapski, A. G. *Acta Chem. Scand.* **1967**, *21*, 661.
(147) Miyasaka, H.; Clerac, R.; Campos-Ferandez, C. S.; Dunbar, K. R. *J. Chem. Soc., Dalton Trans.* **2001**, 858.
(148) Wesemann, J. L.; Chisholm, M. H. *Inorg. Chem.* **1997**, *36*, 3258.
(149) Miyasaka, H.; Campos-Fernandez, C. S.; Clerac, R.; Dunbar, K. R. *Angew. Chem., Int. Ed.* **2000**, *39*, 3831.

CR980024C